ISSN 2096-7071 (Print)
ISSN 2096-3101 (Online)
CN 10-1629/R1

CHINA CDC WEEKLY

Vol. 6 No. 52 Dec. 27, 2024

CDC weekly

中国疾病预防控制中心周报

OCCUPATIONAL HEALTH ISSUE

ISSN 2096-7071
9 772096 707248 52>

Cover Image: credited from the designer Jiaying Wang.

Vital Surveillances

Epidemiological Characteristics and Diagnostic Outcomes of Suspected Occupational Noise-Induced Deafness — Guangdong Province, China, 2014–2023

Shanyu Zhou[1]; Yongshun Huang[1]; Xianzhong Wen[1]; Shu Wang[1]; Bing Xia[1]; Lang Huang[1]; Xudong Li[1,#]

ABSTRACT

Introduction: Suspected occupational noise-induced deafness (ONID) represents the most prevalent suspected occupational disease in Guangdong Province and is among the most frequently reported nationwide. Given its public health significance, we conducted a systematic investigation of suspected ONID cases in Guangdong from 2014 to 2023, analyzing their epidemiological characteristics and diagnostic outcomes to inform evidence-based policies for ONID prevention and management.

Methods: Data on suspected ONID cases reported in Guangdong Province from 2014 to 2023 were extracted from the "Occupational Diseases and Health Hazard Factors Monitoring Information System." Cases were analyzed using descriptive epidemiological methods, with joinpoint regression analysis employed to assess long-term trends.

Results: From 2014 to 2023, 16,987 suspected ONID cases were reported in Guangdong Province, comprising 65.22% of all suspected occupational disease cases (26,044). Cases exhibited a significant increasing trend (Average annual percentage change: 11.8%, 95% *CI*: 2.9%–22.3%, P = 0.013). The Pearl River Delta region accounted for 87.9% of all cases, with manufacturing being the predominant industry (90.1%). Within manufacturing, the metal products industry represented the highest proportion (15.2%). Males constituted 87.7% (14,905/16,987) of cases. Analysis of diagnostic outcomes from 2020 to 2023 revealed an overall diagnostic procedure initiation rate of 45.1%, with a subsequent confirmation rate of 48.9%.

Conclusions: Guangdong Province demonstrates high occurrence patterns of suspected ONID cases, particularly concentrated in the Pearl River Delta region and manufacturing sectors. The low rates of diagnostic procedure initiation and confirmation highlight the urgent need for enhanced regulatory oversight of diagnostic procedures and the development of expert consensus on suspected ONID identification criteria to improve diagnostic confirmation rates.

Occupational noise-induced deafness (ONID) ranks among the most prevalent recognized occupational diseases in industrialized nations (*1*). In China, ONID has maintained its position as the second most common occupational disease since 2015 (*2*), with Guangdong Province reporting it as the leading occupational disease. Suspected ONID represents a preliminary diagnostic state where workers exposed to occupational noise demonstrate hearing loss meeting ONID diagnostic thresholds but require additional exposure documentation or medical evidence for definitive diagnosis (*3*–*4*). The National Health Commission of China emphasizes the importance of enhancing medical institutions' capabilities in identifying suspected occupational diseases and increasing the initiation rate of subsequent diagnostic procedures (*5*). While Guangdong Province reports the highest proportion of suspected ONID cases among suspected occupational diseases provincially and ranks prominently nationwide, comprehensive research examining the epidemiological characteristics and diagnostic outcomes of these cases remains limited (*6*–*7*). To address this knowledge gap, we conducted a systematic investigation of suspected ONID cases in Guangdong Province from 2014 to 2023, analyzing their epidemiological patterns and diagnostic trajectories. This research aims to establish an evidence-based foundation for developing effective ONID prevention and management policies.

METHODS

Surveillance data of suspected ONID cases in

Guangdong Province from January 1, 2014, to December 31, 2023, were extracted from the "Occupational Diseases and Health Hazard Factors Monitoring Information System," a subsystem of the "China Information System for Disease Prevention and Control." All data were de-identified through a unique code assignment. Certified physicians at medical institutions identified suspected ONID cases according to two national standards: the '*Diagnosis of occupational noise-induced deafness (GBZ 49-2014)*' and the '*Identification standard for suspected occupational disease (GBZ 325-2022)*' (*3*–*4*).

The analysis employed descriptive epidemiological methods to characterize suspected ONID cases. The "Occupational Diseases and Health Hazard Factors Monitoring Information System" began collecting data on occupational disease diagnostic procedures in 2020; therefore, epidemiological characteristics analysis encompassed cases from 2014 to 2023, while diagnostic outcome analysis included only cases reported between 2020 and 2023. To ensure a comprehensive assessment of diagnostic progression, cases were followed through June 30, 2024.

The epidemiological analysis examined case distribution across temporal, spatial, and demographic dimensions (sex, age, and occupational noise exposure duration), as well as enterprise attributes (industry sector, scale, and registration type) and identification institution characteristics (ownership type, classification, and certification). Statistical analyses were conducted using R software (version 4.3.0, R Development Core Team). Long-term trends in suspected ONID cases were quantified using Joinpoint regression analysis (Joinpoint software version 5.2.0; National Cancer Institute, Rockville, MD, USA), calculating the annual percentage change (APC) for each segment and the average annual percentage change (AAPC) for the global trend, with corresponding 95% confidence intervals (*CI*s) (*8*). Trends were classified as increasing (APC and/or AAPC>0), decreasing (APC and/or AAPC<0) based on slope significance (P<0.05), or stable (non-significant APC and/or AAPC, P≥0.05) (*9*).

RESULTS

From 2014 to 2023, 16,987 suspected ONID cases were reported, demonstrating a significant increasing trend (AAPC: 11.8, 95% *CI*: 2.9–22.3, P=0.013). Figure 1 depicts the geographic distribution across 21 cities, with the highest case numbers reported in Foshan (3,590; 21.1%), Shenzhen (2,984; 17.6%), Zhongshan (2,400; 14.1%), Dongguan (1,979; 11.7%), and Guangzhou (1,640; 9.7%). The Pearl River Delta region accounted for 87.9% (14,932/16,987) of total cases. The proportion of suspected ONID among all suspected occupational diseases varied substantially by city, ranging from 12.5% in Shanwei to 91.0% in Zhanjiang.

The temporal trends of suspected ONID cases from

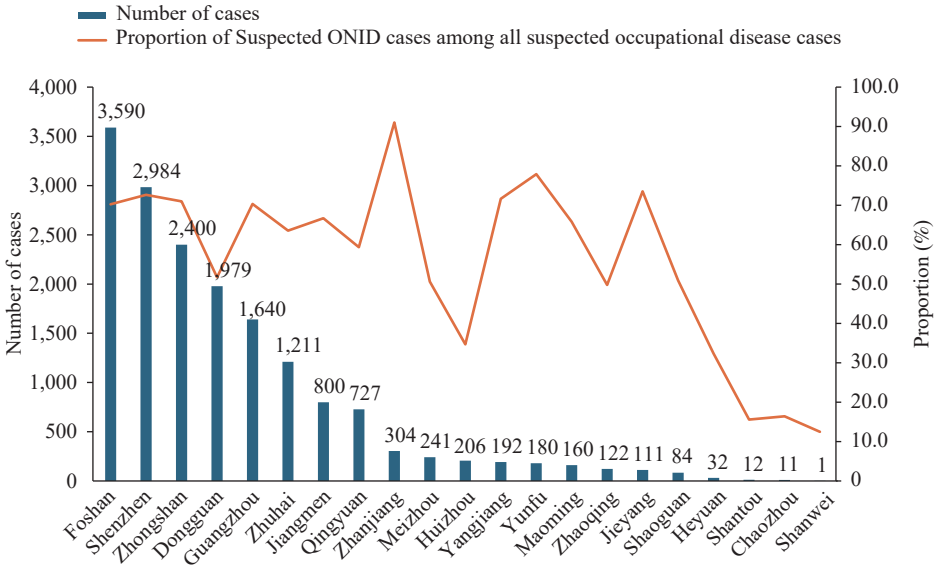

FIGURE 1. Geographic distribution and proportion of suspected occupational noise-induced deafness cases in Guangdong Province, China, 2014–2023.
Abbreviation: ONID=occupational noise-induced deafness.

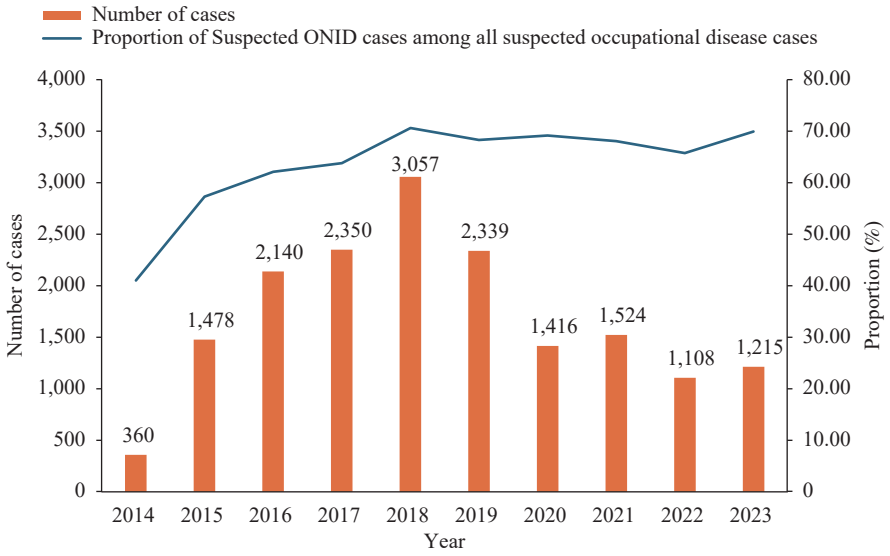

FIGURE 2. Temporal trends and proportional distribution of suspected occupational noise-induced deafness cases in Guangdong Province, China, 2014–2023.
Abbreviation: ONID=occupational noise-induced deafness.

2014 to 2023 are illustrated in Figure 2. Despite fluctuations in absolute numbers, with a peak of 3,057 cases in 2018 followed by a decline to 1,215 cases in 2023, ONID maintained its position as the predominant suspected occupational disease. The proportion of ONID cases increased from 41.05% in 2014 to 70.62% in 2018, and stabilizing between 2019 and 2023. Throughout the decade, suspected ONID cases (16,987) represented 65.22% of all suspected occupational disease cases (26,044).

Table 1 presents the characteristics and AAPC of suspected ONID cases. The manufacturing sector dominated suspected ONID cases, accounting for 90.1% (15,298/16,987) of all reports. Within manufacturing, the metal products industry reported the highest proportion (2,327; 15.2%), followed by non-metallic mineral products (1,416; 9.3%) and electrical machinery and equipment manufacturing (1,314; 8.6%). Domestic-fund enterprises reported 62.1% (10,551/16,987) of cases, demonstrating a significant AAPC of 15.9% (95% *CI*: 4.5%–29.4%, *P*=0.014). Demographic analysis revealed that males comprised 87.7% (14,905/16,987) of cases, with the 40–50 years age group representing 45.2% (7,679/16,987). Cases with <3 years of exposure initially increased from 197 in 2014 to 1,494 in 2018, followed by a marked decline to 33 in 2023 (APC: –52.96%, *P*<0.001 for 2017–2023).

Analysis of identification institution characteristics revealed a notable shift from public to private institutions. While public institutions diagnosed the majority of cases (85.9%; 14,595/16,987), private institutions showed a marked increase in case identification, reaching 34.1% by 2023 (AAPC 107.5%, 95% *CI*: 85.4%–134.0%, *P*<0.001). Hospitals identified 49.0% (8,318/16,987) of cases. The proportion of cases identified by the CDCs decreased from 47.5% to 11.0%, while outpatient health stations exhibited an increased contribution from 0.6% to 18.1% (AAPC=61.5%, 95% *CI*: 29.3%–94.6%, *P*<0.001). Occupational health examination (OHE) institutions identified 72.1% (12,247/16,987) of all cases over the entire study period.

Table 2 demonstrates the diagnostic initiation and confirmation rates for suspected ONID. Among 5,263 suspected cases, the overall diagnostic procedure initiation rate was 45.1%, with a confirmation rate of 48.9%. The initiation rate increased from 36.9% in 2020 to 55.8% in 2022 before decreasing to 47.7% in 2023. Confirmation rates fluctuated between 42.1% and 54.4%, reaching their peak in 2021. Public institutions, which identified 73.1% (3,845/5,263) of cases, demonstrated higher initiation (46.0%) and confirmation (50.7%) rates compared to private institutions (42.8% and 43.8%, respectively). While OHE institutions identified the majority of suspected cases (74.8%, 3,939/5,263), they showed lower initiation (42.5%) and confirmation (46.9%) rates than occupational disease diagnostic institutions (53.0% and 53.8%, respectively). Occupational disease prevention and treatment institutions achieved the

TABLE 1. Characteristics and average annual percentage change of suspected occupational noise-induced deafness cases in Guangdong Province, 2014−2023 (*n*, %).

Characteristics	Total	2014	2015	2016	2017	2018	2019	2020	2021	2022	2023	AAPC (95% *CI*)
Industry												
Manufacturing	15,298 (90.1)	329 (91.4)	1,319 (89.2)	1,901 (88.8)	2,116 (90.0)	2,697 (88.2)	2,121 (90.7)	1,297 (91.6)	1,376 (90.3)	1,032 (93.1)	1,110 (91.4)	11.9* (3.9, 21.5)
Non-Manufacturing	1689 (9.9)	31 (8.6)	159 (10.8)	239 (11.2)	234 (10.0)	360 (11.8)	218 (9.3)	119 (8.4)	148 (9.7)	76 (6.9)	105 (8.6)	10.1 (−3.9, 26.9)
Registration type†												
Domestic-funded enterprises	10,551 (62.1)	176 (48.9)	829 (56.1)	1,205 (56.3)	1,411 (60.0)	2,004 (65.7)	1,444 (61.7)	877 (61.9)	1,041 (68.3)	718 (64.8)	846 (69.7)	15.9* (4.5, 29.4)
Hongkong, Macau and Taiwan-funded enterprises	3,617 (21.3)	96 (26.7)	339 (22.9)	503 (23.5)	489 (20.8)	568 (18.6)	564 (24.1)	333 (23.5)	283 (18.6)	216 (19.5)	226 (18.6)	8.1* (1.4, 15.7)
Foreign-funded enterprises	2,811 (16.5)	88 (24.4)	310 (21.0)	432 (20.2)	450 (19.1)	478 (15.7)	331 (14.2)	206 (14.5)	200 (13.1)	174 (15.7)	142 (11.7)	3.7 (−2.2, 10.4)
Scale†												
Large	2,891 (17.0)	82 (22.8)	326 (22.1)	459 (21.4)	440 (18.7)	460 (15.1)	341 (14.6)	308 (21.8)	207 (13.6)	156 (14.1)	112 (9.2)	3.5 (−3.5, 12.9)
Medium	5,066 (29.8)	134 (37.2)	508 (34.4)	721 (33.7)	688 (29.3)	828 (27.1)	748 (32.0)	348 (24.6)	432 (28.3)	313 (28.2)	346 (28.5)	7.8 (−2.7, 19.9)
Small	7,467 (44.0)	99 (27.5)	493 (33.4)	770 (36.0)	983 (41.8)	1,509 (49.5)	1,090 (46.6)	649 (45.8)	707 (46.4)	550 (49.6)	617 (50.8)	19.9* (10.1, 30.7)
Micro and unknown	1,555 (9.2)	45 (12.5)	151 (10.2)	190 (8.9)	239 (10.2)	253 (8.3)	160 (6.8)	111 (7.8)	178 (11.7)	89 (8.0)	139 (11.4)	8.7 (−12.5, 27.6)
Gender												
Male	14,905 (87.7)	297 (82.5)	1,283 (86.8)	1,843 (86.1)	2,038 (86.7)	2,701 (88.4)	2,029 (86.7)	1,265 (89.3)	1,349 (88.5)	1,002 (90.4)	1,098 (90.4)	12.8* (4.4, 22.6)
Female	2,082 (12.3)	63 (17.5)	195 (13.2)	297 (13.9)	312 (13.3)	356 (11.6)	310 (13.3)	151 (10.7)	175 (11.5)	106 (9.6)	117 (9.6)	5.4 (−6.2, 19.1)
Age (year)												
<30	1,375 (8.1)	67 (18.6)	172 (11.6)	236 (11.0)	243 (10.3)	261 (8.5)	176 (7.5)	69 (4.9)	80 (5.2)	33 (3.0)	38 (3.1)	−10.7* (−16.9, −4.3)
30–39	4,192 (24.7)	116 (32.2)	469 (31.7)	578 (27.0)	629 (26.8)	769 (25.2)	553 (23.6)	318 (22.5)	357 (23.4)	197 (17.8)	206 (17.0)	4.5 (−7.7, 18.3)
40–49	7,679 (45.2)	133 (36.9)	649 (43.9)	986 (46.1)	1,102 (46.9)	1,436 (47.0)	1,111 (47.5)	649 (45.8)	646 (42.4)	493 (44.5)	474 (39.0)	13.1* (5.2, 21.4)
≥50	3,741 (22.0)	44 (12.2)	188 (12.7)	340 (15.9)	376 (16.0)	591 (19.3)	499 (21.3)	380 (26.8)	441 (28.9)	385 (34.7)	497 (40.9)	27.7* (18.8, 39.0)
Duration of occupational noise exposure (year)												
<3	6,076 (35.8)	197 (54.7)	794 (53.7)	1,122 (52.4)	1,268 (54.0)	1,494 (48.9)	875 (37.4)	144 (10.2)	117 (7.7)	32 (2.9)	33 (2.7)	−23.3* (−37.4, −4.4)
3–5	3,682 (21.7)	49 (13.6)	275 (18.6)	340 (15.9)	378 (16.1)	560 (18.3)	491 (21.0)	422 (29.8)	471 (30.9)	332 (30.0)	364 (30.0)	22.4* (10.7, 36.3)
6–8	2,297 (13.5)	46 (12.8)	147 (9.9)	232 (10.8)	229 (9.7)	349 (11.4)	321 (13.7)	264 (18.6)	284 (18.6)	220 (19.9)	205 (16.9)	18.6* (6, 32.6)
≥9	4,932 (29.0)	68 (18.9)	262 (17.7)	446 (20.8)	475 (20.2)	654 (21.4)	652 (27.9)	586 (41.4)	652 (42.8)	524 (47.3)	613 (50.5)	26.1* (17.2, 37.8)
Ownership type of identification institutions												
Public Institution	14,595 (85.9)	360 (100.0)	1,473 (99.7)	2,095 (97.9)	2,215 (94.3)	2,702 (88.4)	1,905 (81.4)	1,154 (81.5)	1,123 (73.7)	767 (69.2)	801 (65.9)	6.7 (−0.9, 15.9)
Private Institution	2,392 (14.1)	0 (0.0)	5 (0.3)	45 (2.1)	135 (5.7)	355 (11.6)	434 (18.6)	262 (18.5)	401 (26.3)	341 (30.8)	414 (34.1)	107.5* (85.4, 134)
Classification of identification institutions												
Occupational Disease Prevention and Treatment Institution	3,187 (18.8)	60 (16.7)	314 (21.2)	585 (27.3)	560 (23.8)	438 (14.3)	328 (14.0)	243 (17.2)	263 (17.3)	215 (19.4)	181 (14.9)	9.9* (4.0, 15.6)
CDC	4,298 (25.3)	171 (47.5)	664 (44.9)	724 (33.8)	612 (26.0)	661 (21.6)	618 (26.4)	315 (22.2)	270 (17.7)	129 (11.6)	134 (11.0)	−4.8 (−16.2, 7.7)
Hospital	8,318 (49.0)	127 (35.3)	467 (31.6)	785 (36.7)	1,082 (46.0)	1,876 (61.4)	1,134 (48.5)	776 (54.8)	812 (53.3)	579 (52.3)	680 (56.0)	15.3* (2.8, 30.8)
Occupational Health Station	1,184 (7.0)	2 (0.6)	33 (2.2)	46 (2.1)	96 (4.1)	82 (2.7)	259 (11.1)	82 (5.8)	179 (11.7)	185 (16.7)	220 (18.1)	61.5* (29.3, 94.6)

Continued

Characteristics	Total	2014	2015	2016	2017	2018	2019	2020	2021	2022	2023	AAPC (95% *CI*)
Certification of identification institutions												
OHE Institution	12,241 (72.1)	250 (69.4)	886 (59.9)	1257 (58.7)	1,618 (68.9)	2,451 (80.2)	1,840 (78.7)	1,058 (74.7)	1,139 (74.7)	788 (71.1)	954 (78.5)	10.5 (−4.8, 28.2)
Occupational Disease Diagnostic Institution	4,746 (27.9)	110 (30.6)	592 (40.1)	883 (41.3)	732 (31.1)	606 (19.8)	499 (21.3)	358 (25.3)	385 (25.3)	320 (28.9)	261 (21.5)	6.4 (−2, 15.5)
Total	16,987 (100.0)	360 (100.0)	1,478 (100.0)	2,140 (100.0)	2,350 (100.0)	3,057 (100.0)	2,339 (100.0)	1,416 (100.0)	1,524 (100.0)	1,108 (100.0)	1,215 (100.0)	11.8* (2.9, 22.3)

Abbreviation: AAPC=Average annual percentage change

* $P<0.05$

† 8 cases from the industry of public administration, social security, and social organizations are not classified by registration type and scale.

TABLE 2. Suspected ONID initiation of occupational disease diagnostic procedure and diagnostic confirmation rates of ONID in Guangdong Province, 2020–2023.

Characteristics	Total of suspected ONID	Initiation of occupational Disease diagnostic procedure			Diagnosis of ONID		
		No	Yes	Initiation rate, %	No	Yes	Diagnostic confirmation rate, %
Year							
2020	1,416	894	522	36.9	242	280	53.6
2021	1,524	868	656	43.0	299	357	54.4
2022	1,108	490	618	55.8	358	260	42.1
2023	1,215	636	579	47.7	314	265	45.8
Ownership type of identification institutions							
Public Institution	3,845	2,077	1,768	46.0	872	896	50.7
Private Institution	1,418	811	607	42.8	341	266	43.8
Certification of identification institutions							
OHE Institution	3,939	2,266	1,673	42.5	889	784	46.9
Occupational disease diagnostic institution	1,324	622	702	53.0	324	378	53.8
Classification of identification institutions							
Occupational disease prevention and treatment institution	902	393	509	56.4	246	263	51.7
CDC	848	446	402	47.4	184	218	54.2
Hospital	2,847	1,688	1,159	40.7	623	536	46.2
Outpatient health station	666	361	305	45.8	160	145	47.5
Total	5,263	2,888	2,375	45.1	1,213	1,162	48.9

Abbreviation: ONID=occupational noise-induced deafness.

highest initiation rate (56.4%), while CDC maintained the highest confirmation rate (54.2%). Although hospitals identified the largest proportion of cases (54.1%, 2,847/5,263), they recorded the lowest initiation (40.7%) and confirmation (46.2%) rates.

DISCUSSION

Throughout the decade from 2014 to 2023, suspected ONID cases maintained a predominant position among occupational diseases in Guangdong Province despite experiencing a decline in absolute numbers after peaking in 2018. This pattern underscores noise as the primary occupational hazard in the region. The geographical distribution revealed that 87.9% of cases were concentrated in the Pearl River Delta, with manufacturing industries accounting for 90.1% of all suspected cases. This concentration aligns with the Pearl River Delta's status as a globally significant manufacturing hub, which inherently concentrates on occupational noise exposure risks (*10*–*11*). The demographic analysis revealed a strong male predominance among cases, attributable to both physiological differences in auditory sensitivity and the higher proportion of males in occupational settings with elevated noise exposure (*12*–*14*). A notable

temporal trend emerged in cases with exposure durations of less than 3 years, showing a sharp decline after 2018. This reduction directly resulted from a clarification issued by the National Health and Family Planning Commission in late 2017, which specified that the 3-year continuous work tenure requirement for ONID diagnosis should be calculated based on calendar days, inclusive of overtime. The institutional landscape evolved significantly during the study period, with occupational health examination institutions increasing from 140 to over 290, marked by substantial growth in private sector participation. By 2023, private institutions conducted 42.5% of occupational health examinations but identified only 34.1% of suspected ONID cases. This discrepancy suggests potential systemic issues, including insufficient technical capacity, inadequate expertise, or suboptimal quality control processes in some private institutions. Furthermore, economic considerations might influence certain private institutions to apply less stringent diagnostic standards, potentially leading to the underdiagnosis of suspected ONID cases (*15*).

Despite an increasing trend in diagnostic procedure initiation rates that peaked in 2022, the overall initiation rate remained low at 45.1%. This improvement reflects enhanced emphasis from health administration authorities and the implementation of the national standard GBZ/T 325-2022, which mandates employers to arrange occupational disease diagnosis within 30 days for suspected cases. However, several factors contribute to the persistently low initiation rate. First, workers with minor hearing impairments often avoid formal diagnosis, fearing that an ONID diagnosis might limit future employment opportunities. Some workers deliberately maintain their "suspected ONID" status to preserve associated benefits. A nationwide study (*16*) revealed that 27.9% of undiagnosed cases were attributed to worker reluctance. Second, informal compensation agreements between employers and workers frequently circumvent the formal diagnostic process. Additionally, some occupational disease identification institutions fail to properly notify workers of their suspected ONID status. Finally, insufficient regulatory enforcement regarding timely diagnostic arrangements by employers remains a significant barrier.

The confirmation rate of 48.9% for suspected ONID cases aligns with the national average of 46.79%(*16*). Initial screening identifies suspected cases based on specific audiometric criteria: binaural high-frequency average hearing threshold (BHFTA) ≥40 dB and a monaural threshold mean value (MTMV) ≥26 dB in the better-hearing ear. However, diagnostic confirmation follows a more stringent protocol requiring a mandatory week-long cessation of noise exposure, followed by three pure-tone audiometry tests conducted at minimum three-day intervals. The final diagnosis adheres to GBZ49-2014 standards, based on the lowest thresholds from these tests. Two primary factors contribute to the relatively low confirmation rate: hearing threshold recovery in borderline cases following noise exposure cessation, and the mandatory requirement of three years' continuous occupational noise exposure. This duration requirement can result in cases where workers exhibit diagnostic-level hearing loss but fail to receive ONID confirmation due to insufficient exposure duration.

A significant disparity in confirmation rates exists between occupational disease diagnostic institutions (53.8%) and OHE institutions (46.9%). This difference likely stems from varying diagnostic approaches: OHE physicians tend to classify cases as suspected ONID when any potential relationship between hearing loss and noise exposure exists, resulting in higher case identification but lower confirmation rates. In contrast, occupational disease diagnostic institutions adhere more rigorously to GBZ 49-2014 criteria, leading to fewer but more precisely identified suspected cases and, consequently higher confirmation rates.

This study had two primary limitations. First, the absence of comprehensive data on the total worker population exposed to occupational noise prevented the calculation of suspected ONID incidence rates. Second, the "Occupational Diseases and Health Hazard Factors Monitoring Information System" only began collecting data on occupational disease diagnostic procedures in 2020, creating a significant data gap that precluded analysis of diagnostic processes for suspected ONID cases from 2014 to 2019 and limited our understanding of long-term diagnostic trends.

In conclusion, our study revealed critical insights into the epidemiological characteristics of suspected ONID in Guangdong Province, demonstrating a persistently high occurrence pattern. Priority attention should be directed toward the Pearl River Delta region, manufacturing industries, and domestic-funded enterprises. These evidence-based findings are essential for guiding targeted and effective resource allocation in ONID prevention and control efforts. Our analysis also highlighted significant concerns, particularly the

low initiation rates of diagnostic procedures and suboptimal diagnostic confirmation rates for suspected ONID cases. To address these challenges, we recommend: 1) developing expert consensus guidelines for identifying suspected ONID; 2) implementing regular quality assessments by health administrative departments; 3) strengthening the capacity and quality control measures of private occupational health examination institutions; 4) conducting comprehensive occupational health promotion activities to enhance awareness of ONID risks and the importance of early diagnosis; and 5) establishing more robust regulatory oversight of diagnostic procedure initiation for suspected ONID cases. These integrated measures are expected to enhance the overall management and prevention of ONID in Guangdong Province and potentially inform occupational health policies throughout China.

Conflicts of interest: No conflicts of interest.

Funding: Supported by the National Key Clinical Specialty Discipline Construction Program of China (2011-09), Guangzhou Science and Technology Bureau Biomedical Industry Innovation Subsidy, Key scientific research projects of Guangdong Province Hospital for Occupational Disease Prevention and Treatment, 2023 Joint Research Center for Institute of Health and Medicine, Hefei Comprehensive National Science Center Research Project (OMH-2023-19), and the Guangdong Special Support Program for Leading Talents.

doi: 10.46234/ccdcw2024.275

[#] Corresponding author: Xudong Li, lixd116@126.com.

[1] Guangdong Province Hospital for Occupational Disease Prevention and Treatment, Guangzhou City, Guangdong Province, China.

Submitted: August 17, 2024
Accepted: December 16, 2024
Issued: December 27, 2024

REFERENCES

1. Lie A, Skogstad M, Johannessen HA, Tynes T, Mehlum IS, Nordby KC, et al. Occupational noise exposure and hearing: a systematic review. Int Arch Occup Environ Health 2016;89(3):351 – 72. https://doi.org/10.1007/s00420-015-1083-5.
2. Sun X. Occupational noise exposure and worker's health in China. China CDC Wkly 2021;3(18):375 – 7. https://doi.org/10.46234/ccdcw2021.102.
3. National Health and Family Planning Commission. GBZ 49-2014 Diagnosis of occupational noise-induced deafness. Beijing: Standards Press of China, 2015. http://www.csres.com/detail/251031.html. (In Chinese).
4. National Health Commission of the People's Republic of China. GBZ/T 325-2022 Identification standard for suspected occupational disease. Beijing: Standards Press of China, 2022. http://www.csres.com/detail/377641.html. (In Chinese).
5. General Office of the National Health Commission, General Affairs Department of the National Administration of Disease Prevention and Control. Notice on further standardizing the management of occupational health examinations and occupational disease diagnosis. https://www.gov.cn/zhengce/zhengceku/202307/content_6890675.htm. [2024-8-16]. (In Chinese).
6. Zhou SY, Wen XZ, Hu SJ, Huang YS, Chen JB. Suspected occupational diseases report and diagnostic situation follow-up in Guangdong Province, 2014-2017. China Occup Med 2018;45(6):708 – 12. https://doi.org/10.11763/j.issn.2095-2619.2018.06.009.
7. Chen YJ, Zhang P, Tang YH, Liu J. Analysis on the incidence and diagnosis of suspected occupational noise- induced deafness in Nanjing from 2015 to 2022. J Southeast Univ (Med Sci Ed) 2023;42(6):865 – 71. https://doi.org/10.3969/j.issn.1671-6264.2023.06.008.
8. Kim HJ, Fay MP, Feuer EJ, Midthune DN. Permutation tests for joinpoint regression with applications to cancer rates. Statist Med 2000;19(3):335 – 51. https://doi.org/10.1002/(SICI)1097-0258(20000215)19:3<335::AID-SIM336>3.0.CO;2-Z.
9. Chen L, Wang LP, Xing Y, Xie JQ, Su BB, Geng MJ, et al. Disparity in spectrum of infectious diseases between in-school and out-of-school children, adolescents, and youths in China: findings from a successive national surveillance from 2013 to 2021. Lancet Reg Health West Pac 2023;38:100811. https://doi.org/10.1016/j.lanwpc.2023.100811.
10. Zhou JN, Shi ZN, Zhou L, Hu Y, Zhang MB. Occupational noise-induced hearing loss in China: a systematic review and meta-analysis. BMJ Open 2020;10(9):e039576. https://doi.org/10.1136/bmjopen-2020-039576.
11. Zhao DY, Feng KS, Sun LX, Baiocchi G, Liu HT. Environmental implications of economic transformation in China's pearl river delta region: dynamics at four nested geographical scales over 1987-2017. Sci Total Environ 2022;816:151631. https://doi.org/10.1016/j.scitotenv.2021.151631.
12. Seixas NS, Neitzel R, Stover B, Sheppard L, Feeney P, Mills D, et al. 10-Year prospective study of noise exposure and hearing damage among construction workers. Occup Environ Med 2012;69(9):643 – 50. https://doi.org/10.1136/oemed-2011-100578.
13. International Organization for Standardization. ISO 1999:2013 Acoustics—Estimation of noise-induced hearing loss. Geneva: ISO. https://www.iso.org/cms/%20render/live/en/sites/isoorg/contents/data/standard/04/51/45103.html?browse=tc.
14. Chen KH, Su SB, Chen KT. An overview of occupational noise-induced hearing loss among workers: epidemiology, pathogenesis, and preventive measures. Environ Health Prev Med 2020;25(1):65. https://doi.org/10.1186/s12199-020-00906-0.
15. Li XY, Huang RY, Xiao MH, Tan XW, Xu LY, Yang AC, et al. Analysis of the on-site quality assessment of occupational medical examination institutions in Guangdong Province in 2023. Chin Occup Med 2024;51(3):308 – 14. https://doi.org/10.20001/j.issn.2095-2619.20240611.
16. Wang D, Li XX, Liu AQ, Wu JH, Wang HF, Hu WJ. Analysis on distribution characteristics and diagnosis of reported suspected occupational diseases in China from 2020 to 2021. Ind Health Occup Dis 2024;50(4):294 – 301. https://doi.org/10.13692/j.cnki.gywsyzyb.2024.04.002.

Preplanned Studies

Prevalence and Risk Factors of Lower Extremity Musculoskeletal Disorders Among Occupational Groups in Key Industries — China, 2018–2023

Ning Jia[1]; Zhongxu Wang[1]; Meibian Zhang[1]; Huadong Zhang[2]; Ruijie Ling[3]; Zhi Wang[4]; Gang Li[5]; Yan Yin[6]; Hua Shao[7]; Jue Li[8]; Hengdong Zhang[9]; Bin Xiao[10]; Hua Zou[11]; Dayu Wang[12]; Yan Ye[13]; Dongxia Li[14]; Jianchao Chen[15]; Enfei Jiang[16]; Bing Qiu[17]; Qiang Zeng[18]; Liangying Mei[19]; Yongquan Liu[20]; Jixiang Liu[21]; Tianlai Li[22]; Jun Qi[23]; Qing Xu[1]; Yang Mimi[1]; Guo Xinwei[1]; Xin Sun[1,#]

Summary

What is already known about this topic?

Lower extremity musculoskeletal diseases (LE-MSDs) have emerged as a significant contributor to the global disease economic burden and worker absenteeism, becoming a global public health concern. However, the epidemic characteristics of LE-MSDs among occupational populations in China are unknown.

What is added by this report?

This report finds that the LE-MSDs prevalence rate among key occupational groups in China is 17.7%, with the top 5 being toy manufacturing, medical personnel, automobile manufacturing, nonferrous metal smelting and rolling processing, and coal mining and washing.

What are the implications for public health practice?

This study investigated the occurrence of LE-MSDs in key industries in China and its possible risk factors to provide big data support for preventing and controlling such diseases in these industries.

Approximately 1.71 billion people worldwide suffer from musculoskeletal diseases (MSDs) (*1*), and this number is expected to increase in the coming decades. The prevention and control of MSDs have attracted global attention. With economic transformation, industrial upgrading, and rapid industrialization in China, new technologies, processes, and materials are widely used, leading to the emergence of new occupational hazards such as MSDs. The Healthy China Action (2019–2030) includes the prevention and control of MSDs caused by adverse ergonomic factors in occupational health protection actions. The National Health Commission of the People's Republic of China is studying the inclusion of MSDs in the Classification and Catalogue of Occupational Diseases and plans to include them in statutory occupational disease management. To provide a solid database for this policy's implementation, the Institute of Occupational Health and Poisoning Control of the China CDC conducted a nationwide risk assessment project from 2018 to 2023. This project focused on studying MSDs caused by adverse ergonomic factors, particularly addressing previous data gaps, such as the lack of comprehensive epidemiological data on the prevalence and risk factors of MSDs in occupational settings and the under-representation of lower extremity MSDs (LE-MSDs) in research. However, lower extremity MSDs (LE-MSDs, including hip/thigh, knee, and ankle/foot) have not received sufficient attention in MSD research and prevention. This may be due to several factors, including a historical focus on upper body MSDs, less recognition of the impact of LE-MSDs on the ability to work and the associated economic burden, and the complexity of diagnosing and attributing LE-MSDs to specific occupational hazards. The global disease burden survey reveals that LE-MSDs have become one of the leading causes of global disabilities (*2*). Therefore, this paper focuses on the distribution of LE-MSDs and related influencing factors in key industries or worker populations in China. This study found that the standardized prevalence rate of LE-MSDs in key industries or occupational groups in China is 17.7%. Individual, work type, and work organization factors may impact LE-MSDs. This study provides data support for China in formulating relevant preventive countermeasures and strategies for MSDs and revising occupational disease classifications and catalogues.

Data for this study were obtained from 7 regions in China: North, East, Central, South, Southwest, Northwest, and Northeast. These regions encompass 9

national economic industries: agriculture, forestry, animal husbandry, fishery, mining, manufacturing, electricity, heat, gas, and water production and supply; construction; wholesale and retail; transportation, warehousing, and postal services; residents' services, repairs, and other services; and health and social work.

This study used stratified random sampling to select representative industries closely related to work-related MSD (WMSD) occurrence from the above-mentioned areas. Samples were drawn according to the following principle: 1–2 large enterprises, 2–4 medium-sized enterprises, and 5–7 small enterprises (all enterprises with insufficient numbers were included). Subsequently, all workers who met the inclusion and exclusion criteria were selected as participants by stratified cluster sampling. Inclusion criteria were workers with >1 year of service. Exclusion criteria were congenital spinal deformity and non-work-related MSDs due to trauma, infectious diseases, and malignant tumors. This study was reviewed by the Medical Ethical Review Committee of Occupational Health and Poison Control at the Chinese Center for Disease Control and Prevention, and all participants provided informed consent.

In this survey, the "Ergonomic Evaluation and Analysis System of WMSDs" (*3*) developed by the Department of Occupational Protection and Ergonomics of the National Institute of Occupational Health and Poison Control of the China CDC was used to investigate the occurrence and influencing factors of WMSDs in key industries or among workers in different regions of China. The survey tool was a questionnaire built into this system, namely, the electronic questionnaire system of the Chinese version of the Musculoskeletal Disorders Questionnaire. This questionnaire was based on the Nordic Musculoskeletal Questionnaire (NMQ) and the Dutch Musculoskeletal Disorders Questionnaire (*4*). After appropriate modification, it has demonstrated good reliability and validity and can be used for occupational populations in China. The survey adopted a 1:N format; one investigator organized N respondents to scan the Quick Response(QR) code of the electronic questionnaire and answer the questions online. Upon completion, questionnaires were directly submitted and uploaded to a cloud database. After export, data were analyzed using SPSS 26.0 (version 26.0; Armonk, NY, USA). The prevalence of LE-MSDs in key industries in China is expressed by the age-standardized prevalence rate based on age composition data (18–60 years old) from the seventh national census. Univariate analysis of LE-MSDs used the χ^2 test, and multivariate analysis used unconditional logistic regression. This study adopted the US National Institute for 0ccupational Safety and Health(NIOSH) criteria (*3*) for LE-MSDs in the United States: discomfort symptoms such as hurt, pain, stiffness, burning, numbness, or tingling, and at the same time: 1) discomfort in the past year; 2) discomfort began after starting the current job; 3) no past accident or sudden injury (in the area of discomfort); and 4) discomfort occurring monthly or lasting more than 1 week was judged as an MSD.

By the end of 2023, 88,609 valid questionnaires were received. Table 1 shows that the standardized prevalence of LE-MSDs in key industries or workers in China was 17.7%, and there were statistically significant differences among industries (P<0.05). The 5 industries with the highest standardized prevalence rates were toy manufacturing (29.0%), medical personnel (25.5%), automobile manufacturing (23.2%), nonferrous metal smelting and rolling processing (22.5%), and coal mining and washing (20.9%).

Individual, work type, and work organization factors may affect LE-MSD prevalence. Univariate analysis (Table 2) identified statistically significant (P<0.05) factors, which were then included as independent variables in a multivariate logistic regression analysis. The results showed that repeatedly performing the same movements with the lower limbs and ankles [odds ratio (*OR*)=1.394, 95% confidence interval (*CI*): 1.325–1.467] was associated with the highest risk of LE-MSDs. Other risk factors included frequently standing at work, job rotation, working in the same postures at a high pace, repetitive trunk movements, staff shortages, frequent overtime work, trunk posture, frequent trunk bending and twisting, prolonged knee bending, frequent squatting or kneeling at work, and exerting significant force with the upper limbs or hands. Protective factors against LE-MSDs included physical exercise, year of investigation, stretching or changing leg posture, frequent sitting at work, and sufficient rest time. Further details are presented in Table 3.

DISCUSSION

Since 2018, the Institute of Occupational Health and Poisoning Control of the China Center for Disease Control and Prevention has organized provincial and municipal centers for disease control and prevention

TABLE 1. Incidence of lower extremity musculoskeletal disorders in key industries or occupational groups in China, 2018–2023. (*n*=88,609).

Industry/working group	Number	Lower extremity musculoskeletal disorders			
		n	pi	p'	95% *CI*
Total	88,609	16,387	18.5	17.7	0.182–0.187
Automobile manufacturing	21,759	5,317	24.4	23.2	0.239–0.250
Computer, communication industry, and other electronic equipment manufacturing	10,638	1,540	14.5	15.4	0.138–0.151
Furniture manufacturing	9,004	1,242	13.8	12.4	0.131–0.145
Footwear industry	7,100	1,036	14.6	15.2	0.138–0.154
Medical staff	7,011	1,899	27.1	25.5	0.260–0.281
Ferrous metal smelting and rolling	3,494	620	17.7	16.3	0.165–0.190
Electrical machinery and equipment manufacturing industry	3,434	343	10.0	9.7	0.090–0.110
Shipping and related device manufacturing	3,431	723	21.1	19.6	0.197–0.224
Coal mining and washing	3,356	735	21.9	20.9	0.205–0.233
Metal products industry	3,195	374	11.7	10.6	0.106–0.128
Nonferrous metal smelting and rolling processing industry	2,312	596	25.8	22.5	0.240–0.276
Road transportation	2,296	254	11.1	14.3	0.098–0.123
Biopharmaceutical product manufacturing	1,738	233	13.4	13.5	0.118–0.150
Railway transportation equipment manufacturing	1,674	220	13.1	12.3	0.115–0.148
Construction	1,434	137	9.6	10.2	0.080–0.111
Civil aviation flight attendants	1,341	270	20.1	18	0.180–0.223
Non-ferrous metal mining and dressing industry	1,225	171	14.0	13.7	0.120–0.159
Comprehensive retail industry	1,086	156	14.4	13.8	0.123–0.165
Food manufacturing industry	828	137	16.5	15.7	0.140–0.191
Automobile repair and maintenance	777	109	14.0	14	0.116–0.165
Toy manufacturing	325	79	24.3	29	0.196–0.290
Animal husbandry	245	48	20.3	20.3	0.146–0.246
Agriculture	239	76	31.8	17.6	0.259–0.377
Cement, lime, and gypsum manufacturing	194	19	9.8	20.4	0.056–0.140
Petrochemical industry	150	8	5.3	4.5	0.017–0.090
Chemical raw materials and chemical products manufacturing industry	95	8	8.4	8.4	0.027–0.141
Handling and warehousing industry	92	7	7.6	6.3	0.021–0.131
Power, heat, gas, water production, and supply	86	20	23.3	18.3	0.141–0.324
Packaging, decoration and other printing industries	50	10	8.1	7.6	0.085–0.315
Chi-square test			1,899.9		
P			*P*<0.001		

Note: pi: actual crude prevalence rate, p': standardised prevalence rate.
Abbreviation: *CI*=confidence interval.

and occupational prevention institutes to conduct occupational health risk assessments of MSDs caused by adverse ergonomic factors in key industries and operations in different regions of China. This project was reported in China Weekly in 2020, 2021, and 2022 (*5*–*7*). The data used in this paper are current to the end of 2023, describe only the occurrence of LE-MSDs, and analyze the related influencing factors.

This study found that the standardized rate of LE-MSDs in key industries or workers in China was 17.7%. In 2015, the European Agency for Safety and Health (EU-OSHA) (*8*) conducted an MSD survey across 28 countries in the European Union using the NMQ. This survey reported a 29% rate of self-reported LE-MSDs. It also showed that the occurrence of LE-MSDs varied across industries, suggesting that

TABLE 2. Univariate analysis of lower extremity musculoskeletal disorders among occupational groups in key industries in China, 2018–2023.

Variables	lower extremity musculoskeletal disorders			
	Number of workers	Case	Percentage (%)	*COR* (95% *CI*)
Individual risk factors				
Gender				
Men	59,989	11,287	18.8	1
Women	28,620	5,100	17.8	0.936 (0.902, 0.970)*
Age (years)				
<25	14,349	2,854	19.90	1
25–34	34,336	6,845	19.90	1.003 (0.955, 1.053)
35–44	22,172	3,827	17.30	0. 840 (0.796, 0.887)*
45–54	13,417	2,180	16.20	0.781 (0.735, 0.831)*
≥55	4,335	681	15.70	0.751 (0.685, 0.823)*
Working age (years)				
<2	22,029	3,534	16.00	1
2–3	17,155	3,204	18.70	1.202 (1.140, 1.267)*
4–5	11,268	2,041	18.10	1.158 (1.090, 1.229)*
6–7	8,414	1,609	19.10	1.237 (1.159, 1.321)*
≥8	29,743	5,999	20.20	1.322 (1.263, 1.384)*
Education level				
Junior high school	27,912	4,067	14.60	1
Senior high school	32,301	6,422	19.90	1.455 (1.394, 1.519)*
University degree	27,157	5,740	21.10	1.571 (1.503, 1.642)*
Graduate degree	1,239	158	12.80	0.857 (0.723, 1.016)
Body mass index (BMI)				
<18.5	7,219	1,426	19.80	1
18.5–24	59,030	10,627	18.00	0.892 (0.839, 0.949)*
≥25	22,360	4,334	19.40	0.977 (0.914, 1.044)
Smoking				
No	55,882	9,981	17.90	1
Occasionally	15,446	2,741	17.70	0.992 (0.947, 1.040)
Frequently	17,281	3,665	21.20	1.238 (1.186, 1.291)*
Physical exercise				
No	27,057	5,400	20.00	1
Occasionally	46,152	8,440	18.30	0.898 (0.864, 0.932)*
Frequently	15,400	2,547	16.50	0.795 (0.755, 0.837)*
Workplace risk factor				
Standing often at work				
No	14,322	1,468	10.20	1
Yes	74,287	14,919	20.10	2.200 (2.079, 2.239)*
Sitting often at work				
No	37,986	8,212	21.60	1
Yes	50,623	8,175	16.10	0.698 (0.675, 0.722)*
Squatting or kneeling often at work				

Continued

Variables	lower extremity musculoskeletal disorders			
	Number of workers	Case	Percentage (%)	*COR* (95% *CI*)
No	53,516	8,064	15.10	1
Yes	35,093	8,323	23.70	1.752 (1.694, 1.813)*
Lift heavy loads (more than 5 kg)				
No	32,171	4,436	13.80	1
Yes	56,438	11,951	21.20	1.680 (1.618, 1.744)*
Lift heavy loads (more than 20 kg)				
No	48,825	7,540	15.40	1
Yes	39,784	8,847	22.20	1.566 (1.513, 1.620)*
Exerting great force on upper limbs or hands				
No	15,302	1,610	10.50	1
Yes	73,307	14,777	20.20	2.147 (2.033, 2.268)*
Use vibration tools at work				
No	55,729	8,639	15.50	1
Yes	32,880	7,748	23.60	1.680 (1.624, 1.739)*
Working in the same postures at a high pace				
No	18,294	1,828	10.00	1
Yes	70,315	14,559	20.70	2.352 (2.234, 2.477)*
Trunk posture				
Trunk straight	30,837	4,158	13.50	1
Bend slightly with your trunk	46,971	8,991	19.10	1.519 (1.459, 1.581)*
Bend heavily with your trunk	10,801	3,238	30.00	2.747 (2.606, 2.895)*
Always turn around with your trunk				
No	33,138	3,951	11.90	1
Yes	55471	12,436	22.40	2.135 (2.054, 2.219)*
Always bend and twist with your trunk				
No	51,769	6,915	13.40	1
Yes	36,840	9,472	25.70	2.245 (2.169, 2.324)*
Always make the same movements with your trunk				
No	44,006	5,262	12.00	1
Yes	44,603	11,125	24.90	2.447 (2.360, 2.536)*
Wrists in bent posture for a prolonged time				
No	37,186	5,150	13.80	1
Yes	51,423	11,237	21.90	1.739 (1.678, 1.803)*
Stretch or change leg posture				
No	20,031	3,885	19.40	1
Yes	68,578	12,502	18.20	0.927 (0.890, 0.964)*
Keep your knees bent for a prolonged time				
No	60,893	9,627	15.80	1
Yes	27,716	6,760	24.40	1.718 (1.659, 1.779)*
Lower limbs and ankles often do the same movements repeatedly				
No	54,101	7,448	13.80	1
Yes	34,508	8,939	25.90	2.190 (2.116, 2.266)*

Continued

Variables	lower extremity musculoskeletal disorders			
	Number of workers	Case	Percentage (%)	*COR* (95% *CI*)
Work organization factors				
Often work overtime	45,009	6,400	14.20	1
No	43,600	9,987	22.90	1.792 (1.731, 1.856)*
Yes				
Abundant resting time				
No	43,384	11,274	26.00	1
Yes	45,225	5,113	11.30	0.363 (0.350, 0.376)*
Decide the rest time independently				
No	69,214	13,757	19.90	1
Yes	19,395	2,630	13.60	0.632 (0.604, 0.662)*
Staff shortage				
No	50,002	6,925	13.80	1
Yes	38,607	9,462	24.50	2.020 (1.951, 2.090)*
Do the same job almost every day				
No	10,530	1,278	12.10	1
Yes	78,079	15,109	19.40	1.737 (1.634, 1.847)*
Job rotation				
No	37,537	5,693	15.20	1
Yes	51,072	10,694	20.90	1.481 (1.430, 1.535)*

Abbreviation: COR=crude odds ratio; *CI*=confidence interval.
* *P*<0.05.

working environments and methods differ. This finding is consistent with the results of the present survey in China.

This study showed that prolonged standing and frequent, repetitive lower limb and ankle movements are high-risk factors for LE-MSDs. Research shows that prolonged standing increases venous pressure in the lower limbs, which may lead to obstructed blood return and venous hypertension (*9*). Persistent venous hypertension not only increases muscle load but also causes poor circulation and insufficient oxygen supply, ultimately leading to muscle fatigue and injury. A laboratory review of prolonged standing and MSDs indicated that standing for 40 minutes can be regarded as the exposure limit for prolonged standing (*10*). In addition to work type, this study found that individual and work organization factors cannot be ignored in relation to LE-MSDs. Studies show that obesity significantly increases the burden on the lower limb musculoskeletal system (*11*). Excess weight places more stress on joints and bones, which can easily cause inflammation, cartilage wear, and muscle injury, particularly in the weight-bearing knee and hip joints. Obesity accelerates tissue degeneration and injury. A survey of female hospital cleaners working under two different organizational models found that the group with more beneficial psychosocial factors (e.g., sufficient staffing, adequate rest time, and fewer shifts) had better musculoskeletal health (*12*). A cross-sectional survey of European working conditions also indicated that good work organization is vital to preventing LE-MSDs (*13*). This aligns with our findings. The following factors may explain this situation. First, frequent overtime and insufficient staffing may lead to prolonged work under high pressure. This continuous physical labor increases the burden on the lower limbs, increasing the risk of LE-MSDs. Additionally, performing the same job almost daily means a lack of variety and restricted movement, leading to the overuse of specific muscle groups and increased musculoskeletal stress due to fixed postures. Conversely, adequate rest time allows employees to recover physically and relieve muscle tension. Short rests promote blood circulation, reduce muscle fatigue, and help prevent MSDs. Self-determination of rest time provides employees with greater flexibility, enabling them to adjust their work rhythm to their physical needs, positively affecting work conditions

TABLE 3. Multivariate logistic regression model predicting the risk factors of lower extremity musculoskeletal disorders among occupational groups in key industries in China, 2018–2021.

Variable	Coefficient	Wald χ^2	*AOR*	95% *CI*	*P*
Lower limbs and ankles often do the same movements repeatedly	0.332	165.193	1.394	1.325, 1.467	0.000
Standing often at work	0.314	63.367	1.368	1.267, 1.478	0.000
Job rotation	0.303	160.727	1.353	1.292, 1.418	0.000
Working in the same postures at a high pace	0.269	42.494	1.309	1.207, 1.419	0.000
Always make the same movements with your trunk	0.266	81.385	1.305	1.232, 1.383	0.000
Staff shortage	0.242	101.516	1.274	1.215, 1.335	0.000
Often work overtime	0.179	57.432	1.196	1.142, 1.253	0.000
Trunk posture	0.13	51.972	1.139	1.099, 1.180	0.000
Always bend and twist with your trunk	0.122	19.711	1.13	1.070, 1.192	0.000
Keep your knees bent for a prolonged time	0.11	17.996	1.117	1.061, 1.175	0.000
Squatting or kneeling often at work	0.107	17.31	1.113	1.058, 1.171	0.000
Exerting great force on upper limbs or hands	0.106	6.739	1.112	1.026, 1.204	0.009
Use vibration tools at work	0.093	14.345	1.097	1.046, 1.151	0.000
Education level	0.087	36.535	1.091	1.061, 1.123	0.000
Body mass index (BMI)	0.077	13.989	1.08	1.037, 1.124	0.000
Working age (years)	0.06	66.734	1.062	1.047, 1.077	0.000
Physical exercise	−0.056	11.116	0.945	0.915, 0.977	0.001
Investigation year	−0.104	195.421	0.901	0.888, 0.914	0.000
Stretch or change leg posture	−0.122	20.834	0.886	0.840, 0.933	0.000
Sitting often at work	−0.258	112.274	0.773	0.737, 0.810	0.000
Abundant resting time	−0.548	465.856	0.578	0.550, 0.608	0.000
Always make the same movements with your trunk	−2.739	1129.345	0.065	0.055, 0.076	0.000

Abbreviation: *AOR*=adjusted odds ratio; *CI*=confidence interval.

and MSD prevention. Implementing a shift system helps break the monotony of work. Varying work hours and task assignments reduce the continuous load on specific muscle groups, thereby reducing the risk of MSDs. Therefore, to protect employee health, companies should consider arranging reasonable working hours, providing sufficient rest opportunities, and implementing shift systems to mitigate MSD risks for employees engaged in the same job long-term.

This study has some limitations. First, as a cross-sectional study, it is subject to recall bias. The study relies on participants' memories of work-related musculoskeletal diseases in the past year, which may be inaccurate. Workers with mild or habitual pain may forget some medical histories and individual cognitive differences can exacerbate inconsistencies in memory quality. Second, causality is uncertain. Although the study identifies related risk factors, the cross-sectional design cannot determine the sequence of variables. Therefore, it is unclear whether working conditions cause the disease or if conditions change after illness onset, which hinders the formulation of effective prevention strategies. In summary, the standardized prevalence rate of LE-MSDs in key industries and occupational groups in China was 17.7%. The five industries or occupational groups with the highest prevalence rates of LE-MSDs are toy manufacturing, medical personnel, automobile manufacturing, nonferrous metal smelting and rolling processing, and coal mining and washing, demonstrating clear occupational characteristics. In addition to occupational factors, such as prolonged standing, personal and work organization factors must also be considered. Therefore, it is necessary to strengthen the dissemination and education of ergonomics knowledge for professionals. These efforts could include improving workbench design, implementing regular rest and activity breaks, and creating personalized exercise prescriptions tailored to the specific needs of the occupational population to reduce the impact of

LE-MSDs in China.

Acknowledgments: All the participants involved in this study, from Chongqing, Shanghai, Jiangsu, Zhejiang, Tianjin, Beijing, Hubei, Ningxia Hui Autonomous Region, Sichuan, Shaanxi and Yunnan Provincial Centers for Disease Prevention and Control, Hubei Provincial Hospital of Integrated Chinese and Western Medicine, Guangzhou Twelfth People's Hospital Affiliated to Guangzhou Medical University, Liaoning Provincial Health Supervision Center, Shenyang, Liaoning, China, Guizhou Province Occupational Disease Prevention and Control Hospital, Shandong Academy of Occupational Health and Occupational Medicine, Guangdong Province Hospital for Occupational Disease Prevention and Treatment, Civil Aviation Medical Center of China Civil Aviation Administration, Tianjin Occupational Disease Prevention and Control Hospital, Fujian Province Occupational Disease and Chemical Poisoning Prevention and Control Center, and Institute of Occupational Medicine of Jiangxi.

Funding: This study was funded by the Project of Occupational Health Risk Assessment and the National Occupational Health Standard Formulation of the National Institute of Occupational Health and Poison Control (Project No. 102393220020 090000020). National Key R&D Program of China (2022YFC2503205).

doi: 10.46234/ccdcw2024.276

[#] Corresponding author: Xin Sun, sunxin@niohp.chinacdc.cn.

[1] National Institute of Occupational Health and Poison Control, Chinese Center for Disease Control and Prevention, Beijing, China; [2] Chongqing Center for Disease Control and Prevention, Chongqing, China; [3] Hubei Provincial Hospital of Integrated Chinese & Western Medicine, Wuhan City, Hubei Province, China; [4] Guangzhou Twelfth People's Hospital Affiliated to Guangzhou Medical University, Guangzhou City, Guangdong Province, China; [5] Liaoning Center for Disease Control and Prevention, Shenyang City, Liaoning Province, China; [6] Shanghai Center for Disease Control and Prevention, Shanghai, China; [7] Shandong Academy of Occupational Health and Occupational Medicine, Jinan City, Shandong Province, China; [8] Beijing Institute of Chemical Industry Occupational Disease Prevention and Treatment, Beijing, China; [9] Jiangsu Provincial Center for Disease Control and Prevention, Nanjing City, Jiangsu Province, China; [10] Guangdong Province Hospital for Occupational Disease Prevention and Treatment, Guangzhou City, Guangdong Province, China; [11] Zhejiang Provincial Center for Disease Control and Prevention, Hangzhou City, Zhejiang Province, China; [12] Tianjin Occupational Disease Prevention and Control Hospital, Tianjin, China; [13] Beijing Center for Disease Control and Prevention, Beijing, China; [14] Guizhou Province Occupational Disease Prevention and Control Hospital, Guiyang City, Guizhou Province, China; [15] Fujian Province Occupational Disease and Chemical Poisoning Prevention and Control Center, Fuzhou City, Fujian Province, China; [16] Sichuan Provincial Center for Disease Control and Prevention, Chengdu City, Sichuan Province, China; [17] Civil Aviation Medical Center, Civil Aviation Administration of China, Beijing, China; [18] Tianjin Center for Disease Control and Prevention, Tianjin, China; [19] Hubei Provincial Center for Disease Control and Prevention, Wuhan City, Hubei Province, China; [20] Institute of Occupational Medicine of Jiangxi, Nanchang City, Jiangxi Province, China; [21] Ningxia Hui Autonomous Region Center for Disease Control and Prevention, Yinchuan City, Ningxia Province, China; [22] Shanxi Provincial Center for Disease Control and Prevention, Xian City, Shanxi Province, China; [23] Yunnan Provincial Center for Disease Control and Prevention, Kunming City, Yunnan Province, China.

Submitted: March 18, 2024
Accepted: November 05, 2024
Issued: December 27, 2024

REFERENCES

1. Cieza A, Causey K, Kamenov K, Hanson SW, Chatterji S, Vos T. Global estimates of the need for rehabilitation based on the Global Burden of Disease study 2019: a systematic analysis for the Global Burden of Disease Study 2019. Lancet 2021;396(10267):2006 – 17. https://doi.org/10.1016/S0140-6736(20)32340-0.
2. Cross M, Smith E, Hoy D, Nolte S, Ackerman I, Fransen M, et al. The global burden of hip and knee osteoarthritis: estimates from the global burden of disease 2010 study. Ann Rheum Dis 2014;73(7):1323 – 30. https://doi.org/10.1136/annrheumdis-2013-204763.
3. Jia N, Zhang MB, Zhang HD, Ling RJ, Liu YM, Li G, et al. Prevalence and risk factors analysis for low back pain among occupational groups in key industries of China. BMC Public Health 2022;22(1):1493. https://doi.org/10.1186/s12889-022-13730-8.
4. Salvendy G. Handbook of human factors and ergonomics. 4th ed. New Jersey: John Wiley & Sons, Inc. 2012. http://dx.doi.org/10.1002/9781118131350.
5. Jia N, Zhang HD, Ling RJ, Liu YM, Li G, Ren ZL, et al. Investigation on work-related musculoskeletal disorders - China, 2018-2019. China CDC Wkly 2020;2(18):299 – 304. https://doi.org/10.46234/ccdcw2020.077.
6. Jia N, Zhang HD, Ling RJ, Liu YM, Li G, Ren ZL, et al. Epidemiological data of work-related musculoskeletal disorders - China, 2018-2020. China CDC Wkly 2021;3(18):383 – 9. https://doi.org/10.46234/ccdcw2021.104.
7. Jia N, Zhang MB, Zhang HD, Ling RJ, Liu YM, Li G, et al. Incidence and risk factors of the upper-limb musculoskeletal disorders among occupational groups in key industries - China, 2018-2021. China CDC Wkly 2022;4(50):1123 – 30. https://doi.org/10.46234/ccdcw2022.227.
8. European Agency for Safety and Health at Work. Work-related musculoskeletal disorders: prevalence, costs and demographics in the EU. European Agency for Safety and Health at Work; 2019 Nov. http://dx.doi.org/10.2802/66947.
9. Antle DM, Côté JN. Relationships between lower limb and trunk discomfort and vascular, muscular and kinetic outcomes during stationary standing work. Gait Posture 2013;37(4):615 – 9. https://doi.org/10.1016/j.gaitpost.2012.10.004.
10. Coenen P, Parry S, Willenberg L, Shi JW, Romero L, Blackwood DM, et al. Associations of prolonged standing with musculoskeletal symptoms-a systematic review of laboratory studies. Gait Posture 2017;58:310 – 8. https://doi.org/10.1016/j.gaitpost.2017.08.024.
11. Wearing SC, Hennig EM, Byrne NM, Steele JR, Hills AP. Musculoskeletal disorders associated with obesity: a biomechanical perspective. Obes Rev 2006;7(3):239 – 50. https://doi.org/10.1111/j.1467-789X.2006.00251.x.
12. Unge J, Ohlsson K, Nordander C, Hansson GÅ, Skerfving S, Balogh I. Differences in physical workload, psychosocial factors and musculoskeletal disorders between two groups of female hospital cleaners with two diverse organizational models. Int Arch Occup Environ Health 2007;81(2):209 – 20. https://doi.org/10.1007/s00420-007-0208-x.
13. Garcia MG, Graf M, Läubli T. Lower limb pain among workers: a cross-sectional analysis of the fifth European Working Conditions Survey. Int Arch Occup Environ Health 2017;90(7):575 – 85. https://doi.org/10.1007/s00420-017-1220-4.

Methods and Applications

Recommended Occupational Exposure Limits for GMA Using Benchmark Dose and Bayesian Model Averaging

Zhihao Chen[1]; Meng Wang[1]; Nankun Liu[1]; Shiyu Wang[1]; Feng Tan[1,#]

ABSTRACT

Introduction: Glycidyl methacrylate (GMA) is a widely used industrial polymerization material. Current occupational exposure limits (OELs) for GMA in China show significant disparities compared to those established by international regulatory bodies, including the United States, the European Union, and Japan. A comprehensive revision of GMA exposure limits is crucial for ensuring optimal worker protection.

Methods: This investigation analyzed data from a 104-week inhalation carcinogenicity study of GMA in mice conducted in Japan. This study identified statistically significant pathological endpoints and employed benchmark dose (BMD) analysis to evaluate meaningful endpoints, focusing on those with the lowest benchmark dose lower bound values. The final recommendations were optimized using Bayesian model averaging (BMA) methodology to establish appropriate OELs.

Results: Our analysis recommends a time-weighted average allowable concentration of 0.01 ppm for GMA, which aligns with international standards established by the European Chemicals Agency (0.016 ppm), Japan Society for Occupational Health (0.012 ppm), and American Conference of Governmental Industrial Hygienists (0.01 ppm).

Conclusion: The combined application of BMD and BMA methodologies represents a scientifically robust approach for deriving points of departure in risk assessment. These evidence-based OELs are essential for effective occupational hazard management and worker health protection.

Glycidyl methacrylate (GMA) serves as a crucial industrial component in composite and epoxy polymer manufacturing and is classified as a high-volume chemical by the Organization for Economic Cooperation and Development screening information dataset (*1*). Following the publication of a 104-week inhalation carcinogenicity study in mice by the Japan Society for Occupational Health (JSOH) in 2015, JSOH (*2*) established an occupational exposure limit of 0.01 ppm for GMA (0.06 mg/m^3, with conversion factors at 25 °C and 760 torr: 1 ppm=5.81 mg/m^3; 1 mg/m^3=0.172 ppm). Subsequently, in 2019, the International Agency for Research on Cancer (IARC) (*2*) classified GMA as a "probable human carcinogen" (Class 2A) based on this study and additional toxicological evidence. This classification prompted JSOH (*3*), the European Chemicals Agency (ECHA)(*4*), and the American Conference of Governmental Industrial Hygienists (*5*) to revise their respective occupational exposure limits (OELs) for GMA to 0.016 ppm and 0.01 ppm. In contrast, China's current occupational exposure limit for GMA remains at a maximum permissible concentration of 5 mg/m^3 (*5*), with no established time-weighted average concentration (PC-TWA). This standard has remained unchanged for over three decades, creating a significant disparity between Chinese regulations and those of Europe, the United States, and Japan.

The regulatory framework for OELs in China differs fundamentally from international standards, as Chinese standards are primarily mandatory rather than recommended guidelines. Given China's specific industrial context, there is an urgent need to develop and revise the OELs for GMA to align with contemporary scientific understanding and international best practices.

The benchmark dose (BMD), introduced by Crump (*6*), represents the statistically derived lower confidence limit of the dose that produces a predetermined benchmark dose response (BMR, typically 1%–10%). This methodology was developed to address significant limitations inherent in the traditional no observed adverse effect level (NOAEL) approach. The scientific committee (SC) endorses the BMD approach as scientifically superior to the NOAEL method for determining a point of departure (PoD)(*7*). In 2017,

the European Food Safety Authority (EFSA)(*8*) published updated guidance recommending model averaging as the preferred methodology for calculating BMD confidence intervals. The SC's updated guidance reaffirms that the BMD approach, particularly model averaging, should be the primary method for deriving PoDs from critical dose-response data when establishing health-based guidance values and margins of exposure.

This investigation aims to establish scientifically robust OELs for GMA through the application of BMD analysis and Bayesian model averaging (BMA) techniques. Our methodology employs BMD analysis to identify potential toxic effect endpoints for GMA, selecting those with the lowest benchmark dose lower bound ($BMDL_{10}$) as critical effects. To enhance the precision and reliability of GMA risk assessment, this study further refined these critical effect outcomes using BMA.

METHODS

Dataset and Endpoint Selection

This investigation utilized data from a 104-week inhalation carcinogenicity study conducted in Japan. The experimental design comprised four groups: three treatment groups and one control group, with 50 female and 50 male rats per group, totaling 400 animals. Subjects were exposed to GMA via inhalation for 6 hours daily, 5 days weekly, throughout the 104-week period. The administered concentrations were 0 (control), 0.6, 2.5, and 10 ppm for both sexes. Detailed study information is accessible at https://anzeninfo.mhlw.go.jp/user/anzen/kag/pdf/gan/0795MAIN.pdf.

Given the absence of definitive human epidemiological evidence for GMA exposure, with existing case reports and occupational investigations lacking precise exposure quantification and being confounded by other potential sensitizing agents, these studies were deemed unsuitable for OEL determination. The selected study adhered to Good Laboratory Practice standards, featured appropriate duration, and employed the relevant exposure route (inhalation), as acknowledged in IARC's assessment. Furthermore, this study serves as the foundational evidence for GMA OELs established by JSOH, ECHA, and other regulatory bodies, validating its selection as the primary toxicological evidence for establishing GMA OELs.

For OEL assessment, chronic toxicity and carcinogenicity were identified as the primary critical effects of GMA. The study results were systematically analyzed, incorporating various uncertainty factors and categorizing endpoints into non-neoplastic and neoplastic lesions, with stratification by sex. Carcinogenicity outcomes were classified by overall and terminal rates, all of which were incorporated into the BMD analysis. Only endpoints demonstrating statistical significance ($P<0.05$) were included in the analysis.

BMD Modeling

The BMD methodology employs statistical models to estimate toxic response probabilities at specified doses, facilitating the identification of dose-response relationships and determination of lower safe doses. Using BMDS software (version 3.3.2, EPA, the United States), this study analyzed statistically significant endpoints ($P\leq0.05$) using nine models: Dichotomous Hill, Gamma, Log-Logistic, Multistage Degree, Weibull, Logistic, Log-Probit, Probit, and Quantal Linear. The BMR level was set at 0.1, with a confidence level of 0.95. The endpoint yielding the lowest $BMDL_{10}$ was selected as the BMD for GMA. Model fit assessment incorporated goodness-of-fit analysis, statistical testing, residual analysis, Akaike information criterion (AIC) value evaluation, *P* value examination, and nested testing.

BMA and Determining PoD

This study utilized BMDS software for modeling key effects. The software assigns prior probabilities to each model based on model selection criteria, with equal default weights assigned to all models. Using binomial sampling for dichotomous endpoints and Normal or Lognormal distributions for continuous data, the software employs Laplace approximation to correct prior density. It then performs BMD estimation through maximum a posteriori probability estimation, computes posterior probabilities across multiple models, and assigns differential weights for model averaging calculations. Bayesian model averaging enhances estimation accuracy by combining results from multiple models. The incorporation of prior information substantially reduces BMD estimation uncertainty and prevents the selection of extreme models that might occur when relying solely on AIC values. By comprehensively evaluating all candidate models, this approach minimizes model

selection bias, thereby improving result accuracy and calculation reliability (*9*).

A PoD represents the dose at which an adverse effect manifests following specific exposure, whether determined empirically or through dose-response modeling (*10*). In our analysis, we employed BMA to assign differential weights across models for averaging calculations and selected the $BMDL_{10}$ as the PoD, following EFSA and EPA recommendations for quantal data.

Application of Uncertainty Factors and Calculation of OEL

Our analysis incorporated uncertainty factors (UFs) for interspecies and intraspecies differences, along with effect severity. This study applied an interspecies factor of 2.5 and, following ECHA recommendations, an intraspecies factor of 5 for worker populations (compared to 10 for general populations) when establishing derived ineffective response levels. For GMA-induced non-neoplastic lesions, which are reversible, this study applied an uncertainty factor of 1. However, given the severity of GMA-induced neoplastic lesions, this study implemented an uncertainty factor of 10.

The final PoD serves as the basis for OEL calculation. Using equal prior probabilities for all models, this study derived GMA OEL values using the following equation:

$$OEL = PoD / UFs$$

where, OEL means occupational exposure limit (ppm); PoD means point of departure; UFs means uncertainty factors.

RESULTS

BMD Analysis Results

Analysis of non-neoplastic lesions in male mice revealed 10 endpoints with $BMDL_{10}$ values ranging from 0.100 to 8.157 ppm. The respiratory metaplasia of the nasal cavity olfactory epithelium yielded the lowest BMDL (0.103 ppm), with optimal fit achieved using the Log-Probit model. In female mice, nine non-neoplastic endpoints produced $BMDL_{10}$ values between 0.077 and 6.825 ppm, with nasopharyngeal eosinophilic change showing the lowest $BMDL_{10}$ (0.077 ppm) using the Dichotomous Hill model. Detailed BMD information is presented in Table 1.

Analysis of tumorigenic endpoints revealed 16 distinct endpoints in male mice, with $BMDL_{10}$ values ranging from 0.756 to 10.197 ppm. The terminal rate of nasal cavity hemangioma demonstrated the lowest $BMDL_{10}$, best fitted by the Dichotomous Hill model. Female mice exhibited 16 neoplastic endpoints with $BMDL_{10}$ values ranging from 0.791 to 7.434 ppm, with uterine histiocytic sarcoma showing the lowest $BMDL_{10}$, optimally fitted using the Log-Logistic model. Table 2 summarizes these findings, which identify the respiratory system as the primary target organ for GMA toxicity in female rats.

BMA Results

Figure 1 illustrates the dose-response relationships derived from Bayesian model averaging across different endpoints. Table 3 presents the posterior probabilities and BMD values post-model averaging. The model averaging approach, which incorporated all viable alternative models while excluding extreme cases, yielded more robust results than classical single-model analysis. For male rats' olfactory epithelial nasal cavity respiratory metaplasia, the Multistage, Quantal Linear, and Weibull models demonstrated superior fit and significantly influenced $BMDL_{10}$ calculations, receiving greater computational weight and yielding a model-averaged $BMDL_{10}$ of 0.118 ppm. Female rats' nasopharyngeal eosinophilia change was best characterized by the Multistage, Quantal Linear, and Log-Logistic models, producing a $BMDL_{10}$ of 0.157 ppm. For mice carcinogenicity endpoints, the Probit, Multistage, and Quantal Linear models provided optimal fit, yielding $BMDL_{10}$ values of 1.733 and 1.081 ppm for males and females, respectively. The lower PoD for non-carcinogenic effects compared to carcinogenic effects indicates that intranasal lesions represent the most sensitive endpoint for GMA inhalation exposure. Application of UFs to the model-averaged results produced OEL values of 0.0094, 0.0126, 0.0139, and 0.0086 ppm, aligning with established limits in the EU (0.016 ppm), Japan (0.012 ppm), and the US (0.01 ppm). Current evidence supports 0.01 ppm as a protective PC-TWA for occupational GMA exposure.

DISCUSSION

This study employed BMD analysis and BMA for GMA risk assessment, utilizing animal studies to identify primary sites of toxic effects. The results demonstrated that GMA's principal adverse effects

TABLE 1. Benchmark dose analysis results of non-neoplastic lesions in mice.

Endpoints	Sex	BMR	Recommended model	*P*	AIC	BMD (ppm)	$BMDL_{10}$ (ppm)
Death	Male	0.1	Log-logistic	0.243	265.728	0.964	0.441
	Female	0.1	–	<0.1	–	–	–
Nasal cavity angiectasis	Male	0.1	Quantal linear	0.968	34.937	16.821	8.157
	Female	0.1	Weibull	1.000	42.496	9.803	6.825
Nasal cavity eosinophilic change: olfactory epithelium	Male	0.1	Log-logistic	0.354	174.269	3.732	2.000
	Female	0.1	Weibull	0.485	221.871	8.783	2.561
Nasal cavity eosinophilic change: respiratory epithelium	Male	0.1	Log-probit	0.578	218.022	1.308	0.435
	Female	0.1	–	<0.1	–	–	–
Nasal cavity respiratory metaplasia: olfactory epithelium	Male	0.1	Log-probit	0.704	189.927	0.256	0.103
	Female	0.1	–	<0.1	–	–	–
Nasal cavity hyperplasia: transitional epithelium	Male	0.1	Multistage degree 3	0.977	86.385	4.505	3.048
	Female		Quantal linear	0.908	49.388	9.380	5.338
Nasal cavity regeneration: respiratory epithelium	Male	0.1	Multistage degree 1	0.730	96.060	3.1808	2.232
	Female	0.1	Gamma	1.000	121.602	1.929	1.166
Nasopharynx eosinophilic change	Male	0.1	Weibull	0.466	141.740	9.471	2.763
	Female	0.1	Dichotomous hill	0.224	227.750	0.294	0.077
Nasal cavity inflammation: respiration epithelium	Male	0.1	Multistage degree 2	0.994	67.035	6.171	4.340
	Female	0.1	–	<0.1	–	–	–
Nasal cavity respiratory metaplasia: gland	Male	0.1	Multistage degree 2	0.819	195.185	0.261	0.194
	Female	0.1	–	<0.1	–	–	–
Nasal cavity squamous cell metaplasia: respiratory epithelium	Male	0.1	–	<0.1	–	–	–
	Female	0.1	Weibull	1.000	61.295	9.388	5.310
Nasa cavity necrosis: olfactory epithelium	Male	0.1	–	<0.1	–	–	–
	Female	0.1	Weibull	0.365	52.707	9.921	6.430
Uterus nodule	Female	0.1	Multistage degree 3	0.968	222.173	8.403	3.053
Ovary enlarged	Female	0.1	Log-probit	0.334	127.124	7.082	2.002

Note: Maximum multistage degree is 3. "-": due to the goodness-of-fit $P<0.1$, the models are poorly fitted and we do not recommend any of them.

Abbreviation: BMR=benchmark response; AIC=akaike information criterion; BMD=benchmark dose; BMDL=benchmark dose lower confidence limit.

manifest at initial exposure sites, specifically the foregut following oral exposure and respiratory tract after inhalation exposure. Chronic GMA exposure in mice induced carcinogenic effects, evidenced by increased tumor incidence in multiple sites including the nasal cavity, lungs, stomach, and uterus. Animal studies (*3*) have also established GMA's reproductive toxicity, while several case reports (*11–12*) have documented allergic reactions in humans exposed to GMA.

The BMD approach demonstrates superior sensitivity compared to the NOAELs/LOAELs methodology, ensuring comprehensive identification of potentially sensitive endpoints for risk assessment. Our analysis yielded $BMDL_{10}$ values of 0.103 and 0.077 ppm as general toxicity PoDs, substantially lower than the NOAEL/LOAEL-derived PoD (0.6 ppm). These results produced OEL values (0.01 ppm) slightly below ECHA's 8h-TWA (0.016 ppm) and JSOH's OEL-M (0.012 ppm). The BMD approach offers distinct advantages: it transcends experimental dose limitations, shows reduced sensitivity to dose spacing, and incorporates both dose-response curve characteristics and statistical uncertainties from data quality. When statistical power is constrained by limited data points or high variability, the BMD approach provides more robust conclusions by considering the complete dose-response curve and addressing statistical limitations more effectively than NOAEL. Consequently, our derived PoD incorporates more comprehensive information and better reflects GMA's actual toxic

TABLE 2. Benchmark dose analysis results of neoplastic lesions in mice.

Site	Tumor	Overall rates			Terminal rates		
		Recommended model	$BMDL_{10}$	AIC	Recommended model	$BMDL_{10}$	AIC
Male							
Nasal cavity	Adenoma	Weibull	9.119	24.697	Weibull	4.612	13.483
	Hemangioma	Dichotomous hill	1.437	72.664	Dichotomous hill	0.756	34.532
	Hemangiosarcoma	Log-probit	4.029	63.888	Weibull	10.197	7.205
	Hemangioma, hemangiosarcoma	Multistage degree 1	2.101	4.815	Dichotomous hill	0.841	36.029
	Hemangioma, hemangiosarcoma, adenoma	Log-probit	2.023	98.715	Quantal linear	1.069	35.197
Lung	Bronchiolar-alveolar adenoma	Weibull	7.626	97.267	Weibull	3.241	45.252
Stomach	Squamous cell papilloma	Weibull	9.245	38.711	Weibull	4.612	13.483
Harderian gland	Adenoma	Log-logistic	4.457	91.079	Log-logistic	1.150	42.070
Female							
Nasal cavity	Hemangioma	Dichotomous hill	1.129	69.193	Multistage degree 1	1.649	22.193
	Hemangiosarcoma	Quantal linear	6.929	40.167	–	–	–
	Hemangioma, hemangiosarcoma	Multistage degree 3	2.797	84.368	Multistage degree 1	1.649	22.193
	Hemangiosarcoma, adenocarcinoma	Quantal linear	6.029	44.961	Weibull	4.947	8.279
	Adenocarcinoma, hemangioma, hemangiosarcoma	Multistage degree 1	2.629	86.773	Weibull	3.973	9.535
Lung	Bronchiolar-alveolar carcinoma	Weibull	7.092	55.751	Weibull	3.973	9.534
	Bronchiolar-alveolar adenoma, bronchiolar-alveolar carcinoma	Weibull	7.434	10.416	Log-logistic	1.447	47.627
Uterus	Histiocytic sarcoma	Logistic	3.448	227.296	Log-logistic	0.791	2.140
Harderian gland	Adenoma	Log-logistic	6.704	68.333	–	–	–

Note: Overall rates represent the number of tumor-bearing animals relative to total animals examined at the site. Terminal rates indicate tumor incidence at terminal kill. Maximum multistage degree is 3. "–": due to the goodness-of-fit $P<0.1$, the models are poorly fitted and we do not recommend any of them.
Abbreviation: AIC=akaike information criterion; BMDL=benchmark dose lower confidence limit.

effect profile. The alignment of final OEL values, despite different methodological approaches (ECHA and JSOH applying a 10-fold uncertainty factor for LOAEL to NOAEL extrapolation), validates 0.01 ppm as a reasonable PC-TWA for GMA under current evidence.

The BMA methodology employed here utilizes a comprehensive dose-response model with weighted mathematical components to calculate model means, generating reliable estimates and confidence intervals. This approach leverages prior information to enhance parameter estimation precision while accounting for model uncertainty. Traditional single-model statistical approaches risk introducing "model selection error (*13*)," which can be mitigated through model averaging techniques (*14*). The method's inherent capacity to address model uncertainty provides enhanced flexibility and reliability in both model selection and parameter estimation (*9*), ultimately establishing a more robust foundation for risk quantification (*7*).

This study was subject to some limitations. The selection of appropriate prior distributions for BMA in BMDS software presents challenges, particularly without comprehensive background knowledge. Furthermore, our reliance on animal test data for OEL recommendations may not fully reflect actual plant operational conditions, necessitating additional field studies for developing more practical OELs.

Our recommended PC-TWA of 0.01 ppm for GMA represents a conservative approach to worker protection. According to ECHA's (*4*) T25 methodology dose-response relationship, this concentration corresponds to approximately 40 additional cancer cases per 100,000 exposed workers. Given GMA's demonstrated high sensitization potential in animal tests and case reports, dermal exposure remains an important area for future research. While modern closed-system manufacturing processes under controlled conditions (*2*) facilitate maintaining low workplace GMA concentrations, current national OELs require revision. Specifically, establishing PC-

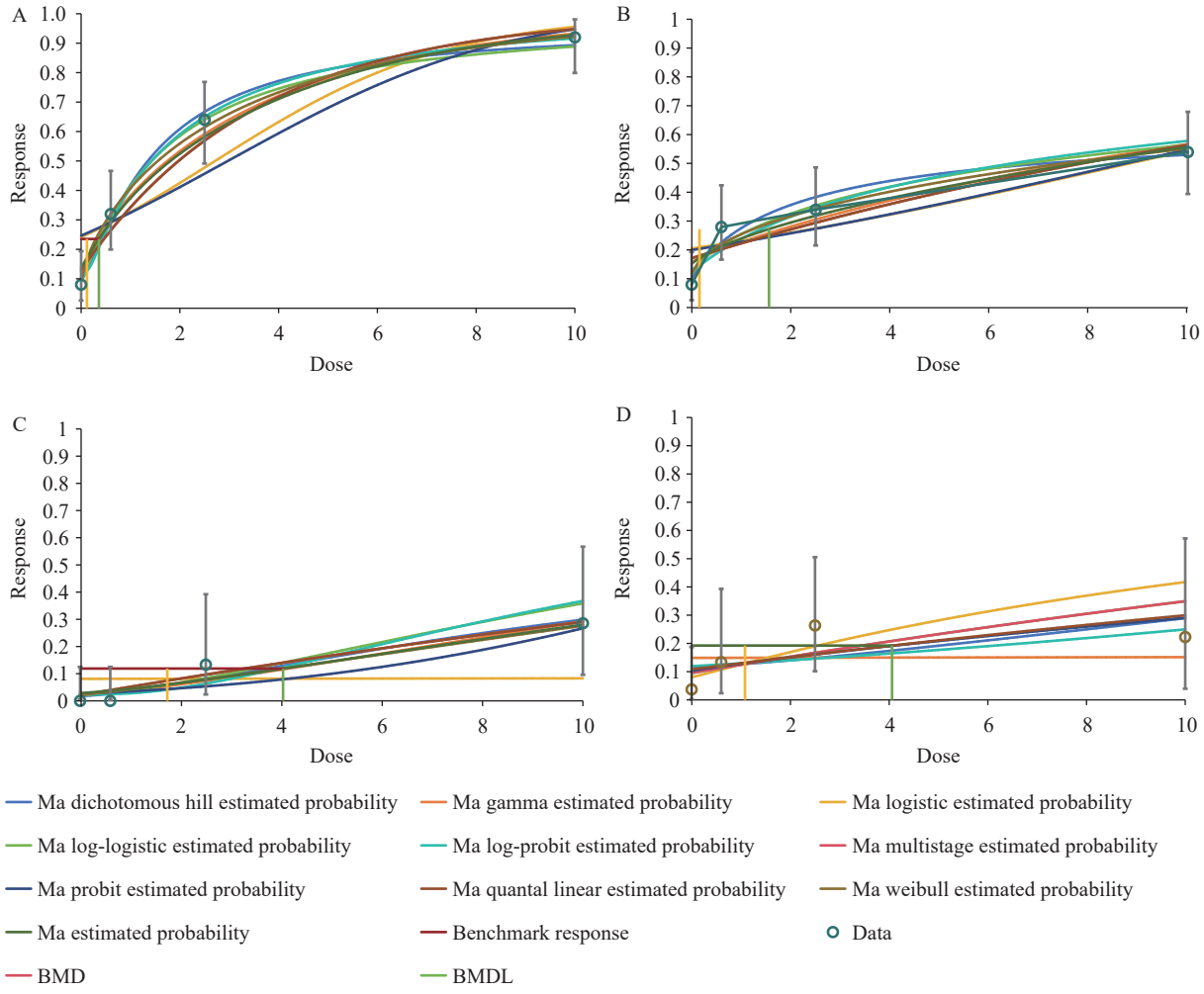

FIGURE 1. Dose-response relationships of bayesian modeling average. (A) Male mice nasal cavity respiratory metaplasia: olfactory epithelium. (B) Female mice Nasopharynx eosinophilic change. (C) Male mice nasal cavity hemangioma. (D) Female mice uterus histiocytic sarcoma.
Abbreviation: Ma=model average; BMD=benchmark dose; BMDL=benchmark dose lower confidence limit.

TABLE 3. Bayesian model averaging results for minimal effect endpoints in mice benchmark dose analysis.

Model	Male mice nasal cavity respiratory metaplasia: olfactory epithelium		Female mice nasopharynx eosinophilic change		Male mice nasal cavity hemangioma		Female mice uterus histiocytic sarcoma	
	Posterior probability	$BMDL_{10}$	Posterior probability	$BMDL_{10}$	Posterior probability	$BMDL_{10}$	Posterior probability	$BMDL_{10}$
Dichotomous hill	0.035	0.119	0.063	0.076	0.155	1.398	–	–
Gamma	0.030	0.064	0.026	0.290	0.061	2.034	0.068	1.248
Logistic	0	0.709	0.041	2.161	0.001	3.714	0.034	6.380
Log-logistic	0.043	0.096	0.092	0.091	0.076	1.575	0.065	0.431
Log-probit	0.023	0.146	0.007	0.176	0.024	1.964	–	–
Multistage	0.391	0.289	0.318	1.112	0.204	1.760	0.274	1.403
Probit	0	0.796	0.061	2.072	0.219	3.994	0.206	3.185
Quantal linear	0.391	0.289	0.318	1.112	0.204	1.760	0.274	1.403
Weibull	0.087	0.053	0.074	0.068	0.057	4.098	0.080	0.518
Model average	–	0.118	–	0.157	–	1.733	–	1.081
OELs value	–	0.0094	–	0.0126	–	0.0139	–	0.0086

Note: Maximum multistage degree is 3. "–": Model not fitted or no data.
Abbreviation: BMDL=benchmark dose lower confidence limit.

TWA and revising maximum allowable concentration are crucial steps toward enhanced worker health protection.

Conflicts of interest: No conflicts of interest.

Funding: Occupational exposure limit for glycidyl methacrylate in workplace air (BZ2023-Q095).

doi: 10.46234/ccdcw2024.277

[#] Corresponding author: Feng Tan, tanfeng@chinacdc.cn.

[1] Chinese Center for Disease Control and Prevention, Beijing, China.

Submitted: October 22, 2024
Accepted: December 01, 2024
Issued: December 27, 2024

REFERENCES

1. OECD. The 2007 OECD list of high production volume chemicals: No.112. 2009. https://one.oecd.org/document/ENV/JM/MONO(2009)40/en/pdf. [2024-10-8].
2. IARC. Some industrial chemical intermediates and solvents. 2020. https://publications.iarc.who.int/Book-And-Report-Series/Iarc-Monographs-On-The-Identification-Of-Carcinogenic-Hazards-To-Humans/Some-Industrial-Chemical-Intermediates-And-Solvents-2020. [2024-10-8].
3. Committee for Recommendation of Occupational Exposure Limits, Japan Society for Occupational Health et al. "Occupational Exposure Limits for ethylidene norbornene, ethyleneimine, benomyl, and 2,3-epoxypropyl methacrylate, and classifications on carcinogenicity." Journal of occupational health vol. 60,4 (2018): 333-335. doi:10.1539/joh.2018-0137-OP
4. ECHA. Occupational exposure limits substance evaluations. 2022. https://echa.europa.eu/oels-activity-list/-/substance-rev/69512/term. [2024-10-09].
5. TLV and BEI Documentation (2023 Documentation)Glycidyl methacrylate. 2022. https://www.acgih.org/wp-content/uploads/2023/04/Glycidyl_Methacrylate.pdf
6. Crump KS. A new method for determining allowable daily intakes. Fundam Appl Toxicol 1874;4(5):854 – 71. https://doi.org/10.1016/0272-0590(84)90107-6.
7. EFSA Scientific Committee, More SJ, Bampidis V, Benford D, Bragard C, Halldorsson TI, et al. Guidance on the use of the benchmark dose approach in risk assessment. EFSA J 2002;20(10):e07584. https://doi.org/10.2903/j.efsa.2022.7584.
8. EFSA Scientific Committee, Hardy A, Benford D, Halldorsson T, Jeger MJ, Knutsen KH, et al. Update: use of the benchmark dose approach in risk assessment. EFSA J 2017;15(1):e04658. https://doi.org/10.2903/j.efsa.2017.4658.
9. Wang YQ. Risk safety assessment of aspartame based on benchmark dose method [dissertation]. Beijing, China: Beijing University of Chemical Technology; 2023. http://dx.doi.org/10.26939/d.cnki.gbhgu.2023.001348. (In Chinese).
10. Maurer LL, Alexander MS, Bachman AN, Grimm FA, Lewis RJ, North CM, et al. An interdisciplinary framework for derivation of occupational exposure limits. Front Public Health 2022;10:1038305. https://doi.org/10.3389/fpubh.2022.1038305.
11. Matura M, Poesen N, de Moor A, Kerre S, Dooms-Goossens A. Glycidyl methacrylate and ethoxyethyl acrylate: new allergens in emulsions used to impregnate paper and textile materials. Contact Dermatitis 1995;33(2):123 – 4. https://doi.org/10.1111/j.1600-0536.1995.tb00514.x.
12. Vogel TA, Christoffers WA, Engfeldt M, Bruze M, Coenraads PJ, Schuttelaar MLA. Severe bullous allergic contact dermatitis caused by glycidyl methacrylate and other acrylates. Contact Dermatitis 2014;71(4):247 – 9. https://doi.org/10.1111/cod.12247.
13. EPA. Benchmark dose technical guidance. 2016. https://archive.epa.gov/raf/web/html/benchmarkdose.html. [2024-10-17].
14. Wheeler MW, Bailer AJ. Comparing model averaging with other model selection strategies for benchmark dose estimation. Environ Ecol Stat 2009;16(1):37 – 51. https://doi.org/10.1007/s10651-007-0071-7.

Methods and Applications

Targeted Analysis of VOCS in Exhaled Breath of Coal Workers' Pneumoconiosis Patients, An Exploratory Study

Rui Gao[1,2,3]; Lijia Yu[1]; Qingyu Meng[1]; Yazhen He[1,2,3]; Fangda Peng[1,2]; Xiangfu Cao[1]; Qingjun Qian[1]; Qicai Liu[1]; Gaisheng Liu[4]; Fan Yang[4]; Yiwei Shi[5]; Qingsong Chen[3]; Chunguang Ding[1,2,3,5,#]

ABSTRACT

Introduction: Pneumoconiosis represents the most prevalent occupational disease in China, with coal workers' pneumoconiosis (CWP) showing the highest incidence. Analysis of volatile organic compounds (VOCs) in the exhaled breath of CWP patients may provide novel insights into its pathogenesis.

Methods: Study data were collected through questionnaires and medical examinations. Thermal desorption-gas chromatography-mass spectrometry was employed for targeted VOC analysis. Differential VOCs were identified using OPLS-DA, the Mann-Whitney U test, and fold change analysis. The discriminatory efficacy of differential VOCs was evaluated using receiver operating characteristic (ROC) curves. Spearman correlation analysis explored relationships between differential VOCs, lung function indices, and blood cell levels.

Results: The pneumoconiosis group showed elevated concentrations of 10 compounds, including isopentane, n-pentane, and isoprene, while four compounds, including 2,4-dimethylpentane, methylcyclohexane, 2,3,4-trimethylpentane, and 2-methylheptane showed decreased concentrations. Combined univariate and multivariate statistical analyses identified six significant VOCs, including isopentane and pentane. Notably, isopentane and n-pentane demonstrated negative correlations with forced vital capacity and levels, while 2-methylheptane showed positive correlations.

Discussion: Clear metabolic differences in VOCs exist between CWP patients and non-dust-exposed healthy controls. Six compounds — isopentane, n-pentane, 3-methylpentane, n-hexane, cyclohexane, and 2-methylheptane — in exhaled breath demonstrate potential as biomarkers for CWP.

Coal Workers' Pneumoconiosis (CWP) is a chronic occupational lung disease that develops following prolonged exposure to mixed coal dust. In China, approximately 15,000 new CWP cases are reported annually. By the end of 2021, the cumulative number of reported occupational pneumoconiosis cases in China reached 915,000, with CWP accounting for 43% of all pneumoconiosis cases. CWP remains a significant public health concern in China, with prevention and treatment challenges persisting. Early screening and diagnosis of CWP represent critical unmet needs in occupational medicine.

The analysis of volatile organic compounds (VOCs) in exhaled breath has emerged as a promising non-invasive diagnostic approach for clinical disease surveillance. Studies have demonstrated that exhaled breath VOCs reflect diverse metabolic processes within the body, with inflammation, oxidative stress, and immune responses significantly influencing both VOC composition and concentration (*1*). VOCs can traverse the air-blood barrier to enter the alveoli, suggesting that exhaled breath VOCs may serve as indicators of systemic metabolic changes, particularly within pulmonary tissue (*2*). This approach has shown promise in biomarker studies for various respiratory conditions, including chronic obstructive pulmonary disease (*3*), idiopathic pulmonary fibrosis (*4*), and lung cancer (*5*). However, research on exhaled breath VOCs in pneumoconiosis remains limited, with previous studies focusing primarily on non-targeted analyses. Notably, no studies have conducted targeted quantitative analyses of exhaled breath from coal workers' pneumoconiosis patients.

Therefore, our study employed thermal desorption-gas chromatography-mass spectrometry (TD-GC-MS) to conduct targeted quantitative analysis of 27 lung disease-associated VOCs in the exhaled breath (alveolar air) of CWP patients. Our objectives were to identify characteristic VOCs for CWP and explore potential biomarkers. We also evaluated the diagnostic potential

of these biomarkers and analyzed their correlations with lung function parameters and blood cell indices.

METHODS

Study Subjects

This study recruited 120 volunteers, of whom 65 met the inclusion and exclusion criteria, with ages ranging from 18 to 80 years. Subjects were excluded if they had: (a) autoimmune diseases, diabetes, cancers, asthma, or other chronic inflammatory conditions; (b) undergone lung lavage or any form of lung surgery; or (c) experienced respiratory infections or taken anti-inflammatory or antibiotic medications within 1 week prior to sampling. Demographic information, including smoking history, alcohol consumption, and previous medical history, was collected for all subjects. Lung function and routine blood test results from physical examinations were obtained, with pulmonary function data calculated as percentages of measured values relative to predicted values. All participants provided written informed consent. This study received approval from the Ethics Committee of the First Hospital of Shanxi Medical University (2020-k-k104).

Sample Collection and Detection

Subjects were instructed to avoid consuming foods with strong odors the day before exhaled breath collection and to fast after 22:00 (including abstaining from smoking and drinking). Sample collection was conducted in a clean, ventilated room maintained at 25 °C (±2 °C) before breakfast. Exhaled breath samples were collected using a Bio-VOC sampler equipped with a one-way valve to capture alveolar air. All thermal desorption (TD) tubes underwent heat pretreatment prior to sampling. During collection, subjects rested seated for 10 minutes before exhaling into a Bio-VOC syringe with a disposable mouthpiece. The collected gas was then transferred to the TD tube, with the process repeated twice to obtain approximately 250 mL of exhaled breath. Two environmental blank samples were collected simultaneously as controls. The thermal desorption tubes were subsequently transported to the laboratory for analysis.

The instrumental methodology has been previously described (*6*). Detailed methodological parameters are provided in Supplementary Table S1 (available at https://weekly.chinacdc.cn/).

Statistical Analysis

Statistical analyses were performed using SPSS 25.0 (IBM, Armonk, New York, USA). The Mann-Whitney U test was employed to detect significant variations in metabolites between groups, with a significance threshold of 0.05. Compounds with $P<0.05$ were incorporated into the lasso regression model using age as a covariate. For compounds below the limit of detection (LOD), concentrations were substituted with LOD/$\sqrt{2}$.

Multivariate statistical analyses were conducted using SIMCA 14.1 (Umetrics, Upsala, Sweden). Initial group differentiation was performed using Principal Component Analysis (PCA) and Orthogonal Partial Least Squares-Discriminant Analysis (OPLS-DA) for visual clustering. Differential VOCs were identified using multiple criteria: variable important in projection (VIP)>1, univariate statistical significance ($P<0.05$), and fold change (FC) >2 or <0.5. Age was included as a covariate, and compounds with univariate statistical significance ($P<0.05$) were incorporated into the Lasso regression model for adjustment. The discriminatory power of screened VOCs was evaluated through receiver operating characteristic (ROC) analysis, with classification ability assessed by area under curve (AUC). Additionally, relationships between variables were examined using Spearman correlation analysis.

Quality Control

Prior to data collection, surveyors underwent rigorous training and assessment to ensure standardization of collection protocols. Sample analyses strictly adhered to established experimental procedures and operational protocols. During data processing and analysis, regular quality checks were performed to identify and remove invalid, duplicate, or inconsistent data entries.

RESULTS

Characteristics of Subjects

The study included 65 participants, comprising 42 CWP patients and 23 healthy controls. Statistical analysis revealed no significant differences between the groups regarding BMI, smoking status, alcohol consumption, and blood indices (Table 1). Analysis of VOC content between groups (Table 2) demonstrated that the CWP group exhibited elevated levels of isopentane, n-pentane, isoprene, 2-methylpentane, 3-methylpentane, 1-hexene, n-hexane, methyl

TABLE 1. Characteristics of subjects.

Variables	CWP (*n*=42)	Control (*n*=23)	*P*
Age (years)	67.6±4.8	47.5±5.7	<0.05
BMI (kg/m^2)	24.8±2.9	26.3±2.5	0.510
Smoking (yes, %)	21 (50.0%)	10 (43.5%)	0.796
Drinking (yes, %)	23 (56.1%)	13 (56.5%)	1.000
FVC (predicted %)	67.083±19.411	85.500±10.117	<0.05
FEV1.0 (predicted %)	79.043±24.699	115.818±11.722	<0.05
WBC (10^9/L)	6.384±1.306	6.571±1.492	0.602
NEU (10^9/L)	4.841±6.723	3.657±0.963	0.406
LYM (10^9/L)	2.059±0.739	2.296±0.755	0.225
NLR	1.948 (1.432, 2.526)	1.559 (1.131, 2.078)	0.072
PLR	107.797 (86.118, 134.303)	116.466 (105.208, 135.795)	0.278

Abbreviation: BMI=body mass index; FVC=forced vital capacity; FEV1.0=forced expiratory volume in one second; WBC=white blood cell; NEU=neutrophil; LYM=lymphocyte; NLR=neutrophil to lymphocyte ratio; PLR=platelet to lymphocyte ratio; CWP=coal workers' pneumoconiosis.

TABLE 2. Quantitative values of VOCs in each group [Median (25th,75th percentile) ppb].

VOC	CWP (*n*=42)	Control (*n*=23)
Iso-pentane*	1.93 (1.004, 3.910)	0.135 (0.069, 0.302)
1-Pentene	0.152 (0.066, 0.541)	0.17 (0.127, 0.268)
Pentane*	2.186 (1.325, 3.373)	0.072 (0.020, 0.180)
Trans-2-Pentene	0.063 (0.063, 0.545)	0.063 (0.063, 0.141)
Iso-prene*	145.904 (105.775, 188.798)	97.534 (63.288, 105.763)
2,2-Dimethylbutane	13.513 (7.003, 20.313)	7.773 (6.345, 22.390)
2-Methylpentane*	0.152 (0.063, 1.724)	0.063 (0.063, 0.133)
3-Methylpentane*	0.511 (0.135, 2.756)	0.091 (0.012, 0.179)
1-Hexene*	0.135 (0.078, 1.145)	0.078 (0.078, 0.254)
Hexane*	1.104 (0.613, 5.399)	0.570 (0.014, 0.900)
2,4-Dimethylpentane*	0.514 (0.176, 1.023)	1.619 (0.902, 2.187)
Methyl-cyclopentane*	0.250 (0.104, 1.317)	0.105 (0.005, 0.235)
2-Methylhexane	0.051 (0.051, 0.070)	0.061 (0.051, 0.086)
Cyclohexane*	0.178 (0.005, 1.155)	0.005 (0.005, 0.025)
2,3-Dimethylpentane	0.120 (0.012, 0.273)	0.043 (0.012, 0.156)
3-Methylhexane	0.045 (0.045, 0.096)	0.196 (0.045, 0.309)
2,2,4-Trimethylpentane	0.017 (0.017, 0.199)	0.017 (0.017, 0.030)
Heptane	0.190 (0.129, 0.538)	0.283 (0.166, 1.324)
Methylcyclohexane*	0.015 (0.005, 0.093)	0.088 (0.032, 0.135)
Pentanal	0.381 (0.185, 1.195)	0.377 (0.181, 0.748)
2,3,4-Trimethylpentane*	0.013 (0.013, 0.013)	0.022 (0.017, 0.027)
2-Methylheptane*	0.039 (0.039, 0.039	0.343 (0.320, 0.442)
3-Methylheptane	0.027 (0.027, 0.027)	0.027 (0.027, 0.027)
4-Methyl-2-pentanone	0.003 (0.003, 3.278)	0.003 (0.003, 0.534)
2-Hexanone*	0.013 (0.013, 0.045)	0.013 (0.013, 0.013)
Hexanal	0.761 (0.369, 1.739)	0.726 (0.517, 0.990)
Decane	0.065 (0.050, 0.187)	0.050 (0.050, 0.072)

Abbreviation: VOC=volatile organic compounds; CWP=coal workers' pneumoconiosis.
* *P*<0.05.

cyclopentane, cyclohexane, and 2-hexanone in exhaled breath compared to controls. Conversely, the CWP group showed decreased levels of 2,4-dimethylpentane, methylcyclohexane, 2,3,4-trimethylpentane, and 2-methylheptane.

Metabolic Profile Analysis

Principal component analysis (PCA), an unsupervised dimensionality reduction technique, was initially employed to visualize the overall data distribution across all samples. The analysis revealed distinct clustering between the pneumoconiosis and control groups based on exhaled VOCs profiles, though with some overlap (Figure 1A). Orthogonal Partial Least Squares-Discriminant Analysis (OPLS-DA), which excels at group discrimination by removing disease-irrelevant information while emphasizing disease-relevant features, demonstrated superior group separation (R^2Y=0.867, Q^2=0.826) as shown in Figure 1B. The model's robustness was validated through 200 permutation tests (Figure 1C), yielding R^2=(0.0, 0.102) and Q^2=(0.0, −0.464), confirming both its validity and reliability.

Screening for Differential VOCs

Differential VOCs were identified using a multi-criteria approach combining VIP values, FC, and statistical significance. The screening criteria included VIP>1, FC>2 or <0.5, and P<0.05 (Supplementary Table S2, available at https://weekly.chinacdc.cn/). This analysis identified six differential VOCs: isopentane, n-pentane, 3-methylpentane, n-hexane, cyclohexane, and 2-methylheptane. Notably, 2-methylheptane maintained statistical significance (P<0.05) after age adjustment in the LASSO regression model.

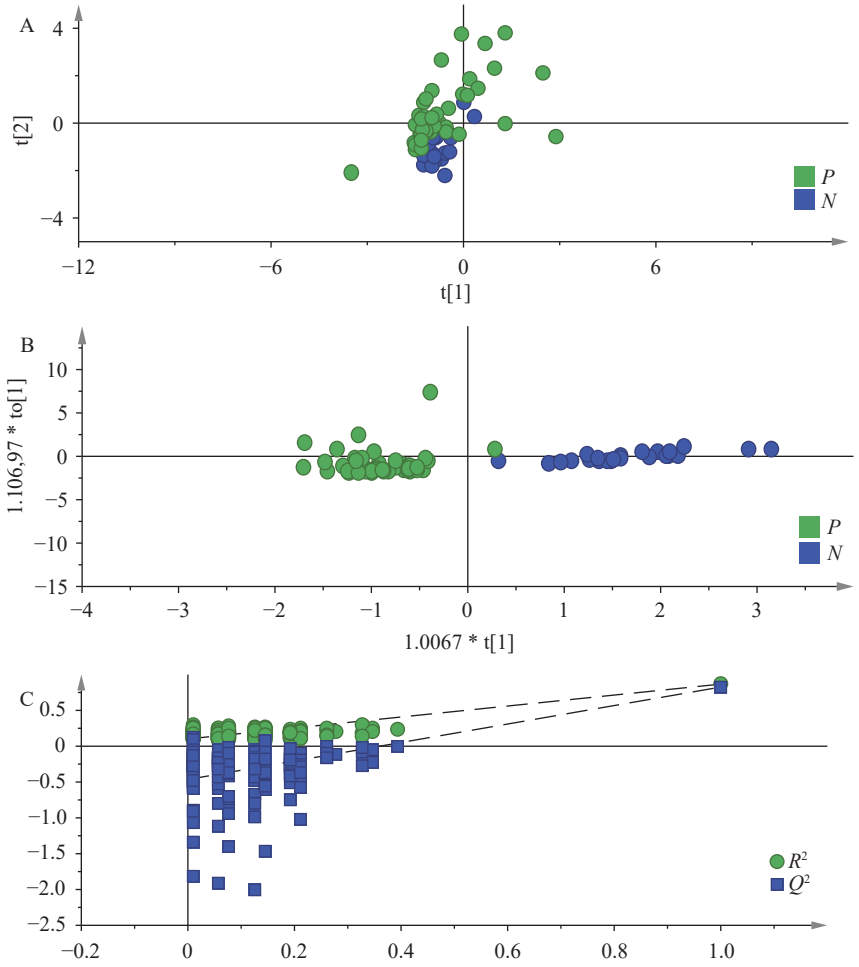

FIGURE 1. Multivariate analysis model. (A) The mode of PCA between coal workers' pneumoconiosis and control group; (B) The mode of OPLS-DA between coal workers' pneumoconiosis and control group; (C) permutation tests of OPLS-DA models for coal workers' pneumoconiosis and control group.
Abbreviation: PCA=principal component analysis; OPLS-DA=orthogonal partial least squares-discriminant analysis.

The diagnostic potential of each differential VOC for CWP was assessed using ROC curves. The AUC values were: isopentane 0.940 [95% confidence interval (*CI*): 0.880, 1.000], n-pentane 0.996 (95% *CI*: 0.986, 1.000), 3-methylpentane 0.776 (95% *CI*: 0.663, 0.889), n-hexane 0.753 (95% *CI*: 0.634, 0.872), cyclohexane 0.777 (95% *CI*: 0.667, 0.888), and 2-methylheptane 0.948 (95% *CI*: 0.878, 1.000). The complete ROC curves and detailed analysis results are presented in Supplementary Figure S1 and Supplementary Table S3 (available at https://weekly.chinacdc.cn/), respectively.

Correlation Between Differential VOCs and Clinical Parameters

Correlation analysis revealed significant associations between the differential VOCs and pulmonary function parameters. Specifically, isopentane and n-pentane demonstrated negative correlations with both FVC (predicted %) and FEV1.0 (predicted %), while 2-methylheptane showed positive correlations with these same parameters (Supplementary Table S4, available at https://weekly.chinacdc.cn/). The relationships between isopentane, n-pentane, and 2-methylheptane versus FVC (predicted %) and FEV1.0 (predicted %) are visually represented in Figure 2.

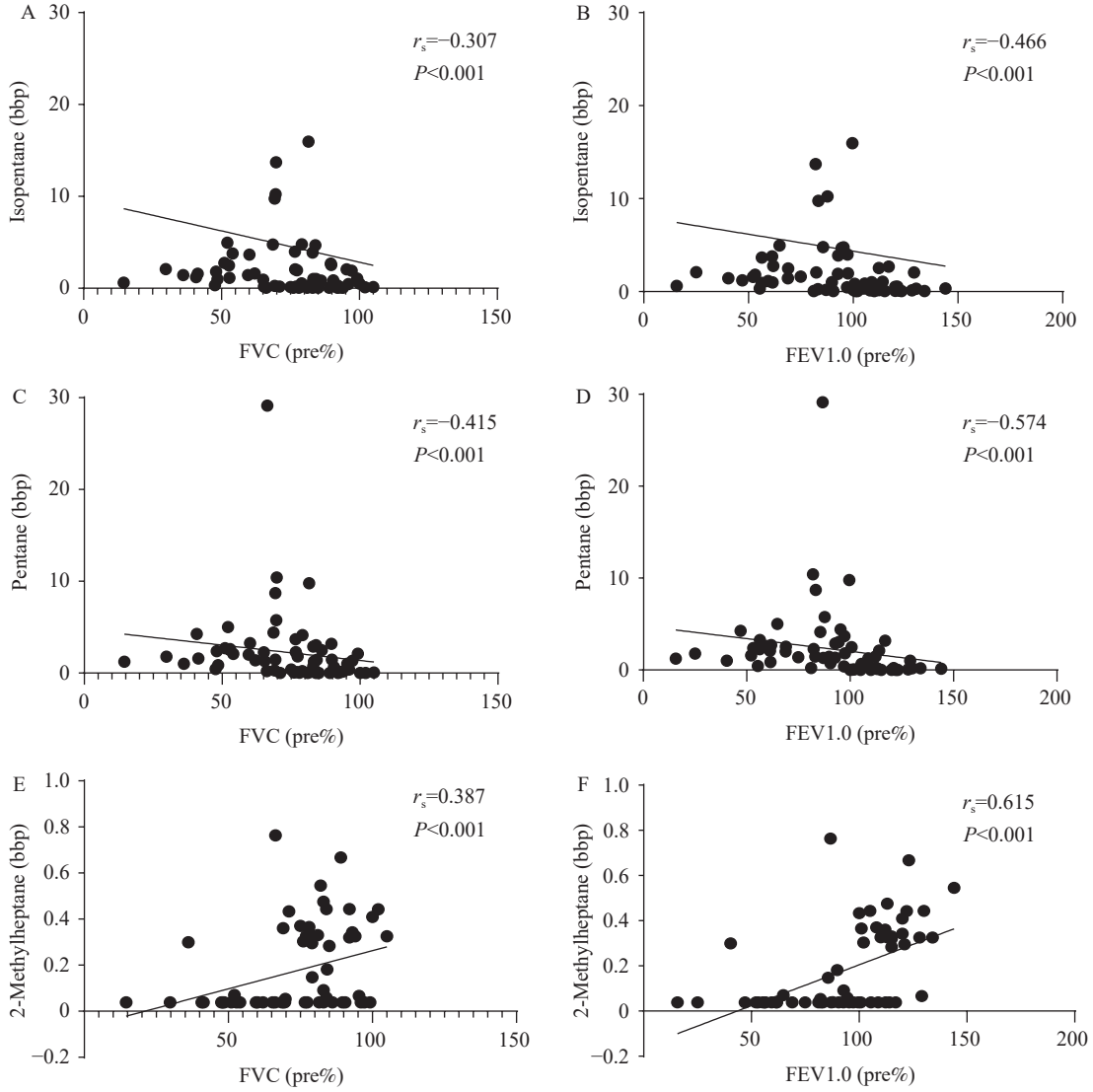

FIGURE 2. Correlation scatterplot. (A) Correlation analysis of isopentane and FVC (pre%); (B) Correlation analysis of isopentane and FEV1.0(pre%); (C) Correlation analysis of pentane and FVC (pre%); (D) Correlation analysis of pentane and FEV1.0 (pre%); (E) Correlation analysis of 2-methylpentane and FVC (pre%); (F) Correlation analysis of 2-methylpentane and FEV1.0 (pre%).
Abbreviation: FVC=forced vital capacity; FEV1.0=forced expiratory volume in one second.

DISCUSSION

In this study, we conducted targeted quantitative analysis using TD-GC-MS technology to analyze exhaled breath samples from 65 subjects. Our findings revealed distinct differences in VOC metabolism between CWP patients and healthy individuals, leading to the identification of six differential VOCs. ROC curve analysis demonstrated that these six VOCs effectively discriminated between the two groups.

In the analysis, elevated isoprene concentrations were observed in the exhaled breath of the coal workers' pneumoconiosis group. Foster (*7*) and colleagues demonstrated that increased exhaled isoprene may be associated with ROS-mediated oxidative stress, suggesting potentially elevated ROS levels in CWP patients. Similarly, pentane concentrations were significantly higher in the CWP group compared to controls. This finding aligns with Jalali (*8*) and colleagues' research, which reported elevated exhaled pentane concentrations in workers exposed to crystalline silica dust, indicating increased oxidative damage to ω-6 polyunsaturated fatty acids in both dust-exposed and affected workers. Furthermore, we observed upregulation of five lipid peroxidation markers — isopentane, n-pentane, 3-methylpentane, n-hexane, and cyclohexane — in the CWP group, suggesting elevated oxidative stress levels. Notably, pentane and hexane have been previously identified as differential diagnostic markers for pneumoconiosis (*9*). The six differential VOCs identified in our study were all alkanes, consistent with these earlier findings.

Furthermore, this study compared clinical indicators between populations and analyzed correlations between the six differential VOCs and clinical parameters. Notably, decreased forced vital capacity (FVC) has been associated with mortality in patients with idiopathic pulmonary fibrosis (IPF) (*10*) and other forms of pulmonary fibrosis, making FVC a critical parameter for assessing disease status in patients with pulmonary fibrosis (*11*). Correlation analyses revealed that isopentane and n-pentane were negatively correlated with FVC and FEV1.0 levels, while 2-methylheptane showed positive correlations with both FVC and FEV1.0 levels ($P<0.05$), suggesting these three VOCs are associated with lung function decline. Importantly, the CWP group exhibited increased concentrations of isopentane and n-pentane and decreased concentrations of 2-methylheptane in exhaled breath, aligning with the correlation analyses and suggesting these three VOCs may serve as potential biomarkers for CWP.

VOCs in the human body originate from both endogenous biochemical processes and environmental exposures, being released through various biological matrices including exhaled breath, urine, and skin (*12*). Exhalation represents the primary release pathway for VOCs in the human body, and its relationship to disease has garnered significant attention, particularly in lung pathologies (*13*). In our study, we identified six differential VOCs in exhaled breath. Analysis using the Human Metabolome Database (HMDB) revealed that cell membranes constitute a primary source for these compounds, with pentane, hexane, cyclohexane, and 2-methylheptane specifically identified as endogenous metabolites in exhaled breath. While the mechanisms underlying endogenous VOC production in human exhaled breath remain incompletely understood, elucidating these production pathways could provide crucial insights into the pathogenesis of coal workers' pneumoconiosis (*14*).

This study has several limitations: First, as an exploratory investigation with a relatively small sample size, future studies with larger cohorts are needed to validate our findings. Second, while previous research has identified methylated alkanes as characteristic VOCs of pneumoconiosis, age significantly influences methylated alkane levels (*15*). Although we included age as a covariate in our analyses, its precise impact on outcomes remains unclear. Future investigations should consider age-matched case-control populations to better control for age-related effects and ensure result reliability.

Conflict of interest: No conflicts of interest.

Funding: Supported by the National Center for Occupational Safety and Health Self-management Project of China (2019009) and the Central Public-Interest Scientific Institution Basal Research Project of China (2020-PT320-005).

doi: 10.46234/ccdcw2024.278

[#] Corresponding author: Chunguang Ding, ding_chg@163.com.

[1] National Center for Occupational Safety and Health, NHC, Beijing, China; [2] NHC Key Laboratory for Engineering Control of Dust Hazard, Beijing, China; [3] Guangdong Pharmaceutical University, Guangzhou City, Guangdong Province, China; [4] Xishan Coal and Electricity (Group) Co., Ltd. Occupational Disease Prevention and Control Center, Taiyuan City, Shanxi Province, China; [5] NHC Key Laboratory of Pneumoconiosis, MOE Key Laboratory of Coal Environmental Pathogenicity and Prevention, Shanxi Key Laboratory of Respiratory Diseases, The First Hospital of Shanxi Medical University, Taiyuan City, Shanxi Province, China.

Submitted: September 06, 2024
Accepted: December 16, 2024
Issued: December 27, 2024

REFERENCES

1. Boots AW, van Berkel JJBN, Dallinga JW, Smolinska A, Wouters EF, van Schooten FJ. The versatile use of exhaled volatile organic compounds in human health and disease. J Breath Res 2012;6(2): 027108. https://doi.org/10.1088/1752-7155/6/2/027108.
2. Di Natale C, Macagnano A, Martinelli E, Paolesse R, D'Arcangelo G, Roscioni C, et al. Lung cancer identification by the analysis of breath by means of an array of non-selective gas sensors. Biosens Bioelectron 2003;18(10):1209 – 18. https://doi.org/10.1016/S0956-5663(03)00086-1.
3. Li ZT, Zeng PY, Chen ZM, Guan WJ, Wang T, Lin Y, et al. Exhaled volatile organic compounds for identifying patients with chronic pulmonary aspergillosis. Front Med 2021;8:720119. https://doi.org/10.3389/FMED.2021.720119.
4. Yamada YI, Yamada G, Otsuka M, Nishikiori H, Ikeda K, Umeda Y, et al. Volatile organic compounds in exhaled breath of idiopathic pulmonary fibrosis for discrimination from healthy subjects. Lung 2017;195(2):247 – 54. https://doi.org/10.1007/s00408-017-9979-3.
5. Zou YC, Wang Y, Jiang ZL, Zhou Y, Chen Y, Hu YJ, et al. Breath profile as composite biomarkers for lung cancer diagnosis. Lung Cancer 2021;154:206 – 13. https://doi.org/10.1016/j.lungcan.2021.01.020.
6. Gao R, Peng FD, He YZ, Feng J, Liu WB, Yu LJ, et al. Determination of 27 volatile organic compounds in exhaled breath bythermal desorption-gas chromatography-mass spectrometry. J Environ Occup Med 2024;41(1):96 – 102. https://doi.org/10.11836/JEOM23283.
7. Foster WM, Jiang L, Stetkiewicz PT, Risby TH. Breath isoprene: temporal changes in respiratory output after exposure to ozone. J Appl Physiol (1985) 1996;80(2):706-10. http://dx.doi.org/10.1152/jappl.1996.80.2.706.
8. Jalali M, Zare Sakhvidi MJ, Bahrami A, Berijani N, Mahjub H. Oxidative stress biomarkers in exhaled breath of workers exposed to crystalline silica dust by SPME-GC-MS. J Res Health Sci 2016;16(3): 153 – 61.
9. Yang HY, Shie RH, Chang CJ, Chen PC. Development of breath test for pneumoconiosis: a case-control study. Respir Res 2017;18(1):178. https://doi.org/10.1186/s12931-017-0661-3.
10. Collard HR, King Jr TE, Bartelson BB, Vourlekis JS, Schwarz MI, Brown KK. Changes in clinical and physiologic variables predict survival in idiopathic pulmonary fibrosis. Am J Respir Crit Care Med 2003;168(5):538 – 42. https://doi.org/10.1164/rccm.200211-1311OC.
11. Takei R, Brown KK, Yamano Y, Kataoka K, Yokoyama T, Matsuda T, et al. Prevalence and prognosis of chronic fibrosing interstitial lung diseases with a progressive phenotype. Respirology 2022;27(5):333 – 40. https://doi.org/10.1111/resp.14245.
12. Drabińska N, Flynn C, Ratcliffe N, Belluomo I, Myridakis A, Gould O, et al. A literature survey of all volatiles from healthy human breath and bodily fluids: the human volatilome. J Breath Res 2021;15(3): 034001. https://doi.org/10.1088/1752-7163/abf1d0.
13. van der Schee MP, Paff T, Brinkman P, van Aalderen WMC, Haarman EG, Sterk PJ. Breathomics in lung disease. Chest 2015;147(1):224 – 31. https://doi.org/10.1378/chest.14-0781.
14. Magnano MC, Ahmed W, Wang R, Bergant Marušič M, Fowler SJ, White IR. Exhaled volatile organic compounds and respiratory disease: recent progress and future outlook. TrAC Trends Anal Chem 2024;176:117739. https://doi.org/10.1016/j.trac.2024.117739.
15. Phillips M, Cataneo RN, Greenberg J, Gunawardena R, Rahbari-Oskoui F. Increased oxidative stress in younger as well as in older humans. Clin Chim Acta 2003;328(1-2):83 – 6. https://doi.org/10.1016/S0009-8981(02)00380-7.

SUPPLEMENTARY MATERIAL

SUPPLEMENTARY TABLE S1. Linear equations, correlation coefficients, measurement ranges, detection limits and quantification limits for VOCs.

VOC	LOD/(ppb)	LOQ/(ppb)
Iso-pentane	0.098	0.326
1-Pentene	0.094	0.312
Pentane	0.028	0.092
Trans-2-Pentene	0.089	0.297
Iso-prene	0.015	0.049
2,2-Dimethylbutane	0.133	0.444
2-Methylpentane	0.089	0.297
3-Methylpentane	0.017	0.058
1-Hexene	0.110	0.367
Hexane	0.019	0.065
2,4-Dimethylpentane	0.111	0.370
Methylcyclopentane	0.007	0.025
2-Methylhexane	0.071	0.238
Cyclohexane	0.006	0.022
2,3-Dimethylpentane	0.017	0.057
3-Methylhexane	0.064	0.214
2,2,4-Trimethylpentane	0.024	0.080
Heptane	0.073	0.244
Methylcyclohexane	0.007	0.023
Pentanal	0.067	0.225
2,3,4-Trimethylpentane	0.018	0.061
2-Methylheptane	0.055	0.182
3-Methylheptane	0.038	0.126
4-Methyl-2-pentanone	0.005	0.015
2-Hexanone	0.018	0.060
Hexanal	0.070	0.233
Decane	0.070	0.234

Abbreviation: LOD=limit of detection; LOQ=limit of quantification; VOC=volatile organic compounds.

SUPPLEMENTARY TABLE S2. Screening for differential VOCs.

VOC	VIP	FC(N/P)	*P*	Adjusted p-value
Iso-pentane	1.931	0.028	<0.05	1.000
1-Pentene	0.076	0.235	0.454	–
Pentane	2.314	0.035	<0.05	0.530
Trans-2-Pentene	0.529	0.471	0.293	–
Iso-prene	1.237	0.637	<0.05	0.938
2,2-Dimethylbutane	0.129	0.957	0.358	–
2-Methylpentane	0.848	0.019	<0.05	1.000
3-Methylpentane	1.190	0.016	<0.05	1.000
1-Hexene	0.549	0.330	<0.05	0.977
Hexane	1.090	0.017	<0.05	1.000
2,4-Dimethylpentane	1.226	1.511	<0.05	1.000
Methylcyclopentane	0.989	0.035	<0.05	1.000
2-Methylhexane	0.278	0.391	0.292	–
Cyclohexane	1.235	0.015	<0.05	1.000
2,3-Dimethylpentane	0.510	0.237	0.562	–
3-Methylhexane	0.290	0.210	0.158	–
2,2,4-Trimethylpentane	0.696	0.117	0.362	–
Heptane	0.494	0.750	0.079	–
Methylcyclohexane	0.725	0.484	<0.05	1.000
Pentanal	0.109	0.755	0.661	–
2,3,4-Trimethylpentane	0.659	1.047	<0.05	1.000
2-Methylheptane	2.238	5.161	<0.05	0.014*
3-Methylheptane	0.382	0.432	0.355	–
4-Methyl-2-pentanone	0.518	0.055	0.182	–
2-Hexanone	0.652	0.247	<0.05	1.000
Hexanal	0.079	0.700	0.671	–
Decane	0.688	0.388	0.285	–

Abbreviation: VOC=volatile organic compounds; VIP=variable importance in projection; FC=fold change; N=control group; P=coal workers' pneumoconiosis group.
* *P*<0.05.

SUPPLEMENTARY TABLE S3. ROC curve results for six differential VOCs.

VOC	AUC	95% *CI*	Sensitivity	Specificity	Cut-off value	*P*
Isopentane	0.940	0.880–1.000	0.881	1.000	0.5733	<0.001
Pentane	0.996	0.986–1.000	0.976	1.000	0.4227	<0.001
3-Methylpentane	0.776	0.663–0.889	0.738	0.783	0.1887	<0.001
Hexane	0.753	0.634–0.872	0.762	0.696	0.6565	<0.001
Cyclohexane	0.777	0.667–0.888	0.643	0.913	0.1101	<0.001
2-Methylheptane	0.948	0.878–1.000	0.952	0.956	0.2330	<0.001
Combined	1.000	1.000–1.000	1.000	1.000	–	<0.001

Abbreviation: VOC=volatile organic compounds; AUC= area under curve; CI=confidence interval.
* *P*<0.05.

SUPPLEMENTARY TABLE S4. Correlation between differential VOCs and clinical parameters.

VOC		WBC	NEU	LYM	NLR	PLR	FVC (predicted %)	FEV1.0 (predicted %)
Isopentane	r_s	−0.017	0.095	−0.08	0.171	−0.033	−0.307	−0.466
	P	0.895	0.454	0.528	0.173	0.793	0.014*	<0.001*
Pentane	r_s	0.039	0.158	−0.003	0.177	−0.111	−0.415	−0.574
	P	0.759	0.208	0.981	0.158	0.377	0.001*	<0.001*
3-Methylpentane	r_s	0.025	0.101	−0.040	0.131	−0.029	−0.143	−0.193
	P	0.844	0.422	0.753	0.297	0.820	0.261	0.127
Hexane	r_s	−0.015	0.08	−0.063	0.129	0.032	−0.064	−0.140
	P	0.904	0.525	0.618	0.306	0.799	0.615	0.270
Cyclohexane	r_s	−0.059	0.008	−0.042	0.061	−0.044	−0.098	−0.160
	P	0.642	0.948	0.739	0.628	0.728	0.439	0.205
2-Methylheptane	r_s	0.053	−0.082	0.126	−0.223	0.115	0.387	0.615
	P	0.677	0.515	0.316	0.074	0.361	0.002*	<0.001*

Abbreviation: WBC=white blood cell; NEU=neutrophil; LYM=lymphocyte; NLR=neutrophil to lymphocyte ratio; PLR=platelet to lymphocyte ratio; FVC=forced vital capacity; FEV1.0=forced expiratory volume in one second; VOC=volatile organic compounds.
* indicates $P<0.05$.

Methods and Aplications

Coal Worker's Pneumoconiosis-Targeted Lipidomics Reveals Aberrant Phospholipid Metabolism for Early-Stage Diagnosis

Yuzhen Feng[1,2,3]; Jing Dai[2,3]; Junyun Wang[2,3]; Fangda Peng[2,3]; Wenrong Wang[2,3,4]; Xiao Yu[5]; Xiaomei Kong[5]; Qingjun Qian[2,3]; Qicai Liu[2,3]; Huanqiang Wang[4]; Chunguang Ding[1,2,3,#]; Yiwei Shi[5,#]

ABSTRACT

Introduction: Pneumoconiosis is the most prevalent occupational disease in China, with coal worker pneumoconiosis (CWP) demonstrating the highest incidence. Studies have indicated that phospholipids may be associated with CWP.

Methods: In this study, serum was obtained from 62 patients with pneumoconiosis, 105 coal dust-exposed workers, and 50 healthy individuals and analyzed via targeted lipidomics using ultra-performance liquid chromatography-tandem mass spectrometry (UPLC-MS/MS). After initially identifying phospholipids with significant differences through univariate and multivariate statistical analyses, receiver operating characteristic (ROC) analysis was performed. The differential phospholipids identified in patient samples were then integrated to assess their diagnostic potential for CWP using a support vector machine (SVM).

Results: Compared with healthy subjects, the levels of Lyso-PS (18:0) were decreased, while PC (16:0), PC (18:0), PC (16:0/18:1), PI (16:0/18:1), PS (18:1), PG (16:0), and PG (18:0/18:1) were significantly increased in the pneumoconiosis group, with an area under the curve (AUC)>0.7. Moreover, compared with the dust-exposed group, Lyso-PC (16:0), PC (16:0), PC (16:0/18:1), PI (16:0/18:1), and PG (16:0) were significantly elevated in the pneumoconiosis group, with an AUC>0.7. The diagnostic model, including PC (16:0), PC (16:0/18:1), PI (16:0/18:1), and PG (16:0), demonstrated excellent performance with an AUC of 0.956.

Discussion: The serum phospholipid profiles of patients with pneumoconiosis differed significantly from those of controls, including differences in PC, Lyso-PC, PI, PS, Lyso-PS, and PG. Among these, a diagnostic model incorporating PC (16:0), PC (16:0/18:1), PI (16:0/18:1), and PG (16:0) demonstrated superior screening efficiency.

Coal worker pneumoconiosis (CWP) results from prolonged dust inhalation by miners and remains incurable. Despite a decline in the overall incidence of pneumoconiosis, it remained the most prevalent occupational disease in 2022, accounting for 68% of cases and 9,613 deaths, according to the National Health Commission statistical bulletin.

Evidence suggests a strong link between lipid metabolism and pulmonary fibrosis. For instance, mice deficient in the *Elovl6* gene exhibit altered lung lipid profiles and an exacerbated fibrotic response to bleomycin (*1*). Phospholipids, the primary constituents of pulmonary surfactants, demonstrate cell type-specific distributions within the lung: phosphatidylglycerol (PG) and phosphatidylcholine (PC) predominate in alveolar cells, phosphatidylethanolamine (PE) in macrophages, and phosphatidylinositol (PI) in bronchial epithelial cells. Dysregulation of phospholipid homeostasis can trigger myofibroblast activation, extracellular matrix deposition, and ultimately, fibrosis (*2*). Moreover, oxidized phospholipids may contribute to inflammation following lung injury. Impaired phosphatidylcholine secretion, for example, has been shown to promote M2 macrophage reprogramming and fibrosis (*3*). Similarly, knockdown of autotaxin in bronchial epithelial cells or macrophages attenuates collagen accumulation after bleomycin exposure (*4*). Collectively, these findings underscore the multifaceted roles of phospholipids in cellular structure, inflammatory responses, and the regulation of oxidative stress.

Studies have shown that phospholipids are closely linked to the inflammatory process of pulmonary fibrosis and may serve as potential diagnostic biomarkers (*5*–*6*). However, the literature on phospholipid alterations in CWP and their potential as CWP biomarkers remains limited.

In summary, this study conducted targeted lipidomics analysis of 22 disease-related phospholipids using UPLC-MS/MS to evaluate their potential as serum biomarkers for CWP (*7*).

METHODS

Study Subjects and Sample Collection

A total of 217 subjects were recruited, including 62 stage I CWP patients (PN group) from a Beijing coal mine, 50 healthy volunteers (HT group), and 105 environmental control group members (EX group). All subjects were aged 40–55 years with a BMI of 18.5–30.0 kg/m^2. Pneumoconiosis diagnoses were confirmed by three occupational physicians according to the "Diagnostic Criteria of Pneumoconiosis" in China. The EX group consisted of coal mine dust-exposed workers sharing the same environment as the PN group and at high risk for pneumoconiosis, while healthy volunteers were matched to the patients by age and sex. Exclusion criteria included COPD, asthma, tuberculosis, or cancer. Lung function tests (FVC, FEV1, MMEF) for the PN and EX groups were conducted following Chinese Thoracic Society guidelines. Subjects with hypertension, arthritis, or gastritis were categorized as having chronic conditions. Serum was separated from 5 mL blood samples and then stored at −80 °C.

Detection of Lipidomics in UPLC-MS/MS

Our research team established a targeted lipidomics approach using a UPLC-MS/MS system (Waters Corp., USA) with electrospray ionization (ESI). The mobile phase consisted of methanol/water (5:95, v/v) with 10 mmol/L ammonium formate (Solvent A) and methanol (Solvent B), at a flow rate of 0.4 mL/min and an injection volume of 5 μL. Details of the mobile phase gradient and multiple reaction monitoring (MRM) parameters are available in our previous study (*7*). Quality control (QC) samples were analyzed every 30 samples during the run.

Statistical Analysis

Statistical analyses were performed using IBM SPSS Statistics 25 (International Business Machines Corporation, New York, USA.) and R 4.3.2 (supported by The R Foundation for Statistical Computing, Vienna, Austria). The Student's *t*-test and Mann-Whitney *U* test were used for continuous variables, depending on data distribution, while Pearson's χ^2 test assessed categorical variables. *P* values were adjusted for the False Discovery Rate (FDR) using the Benjamini-Hochberg method and reported as *q* values. Data are presented as means±standard deviation (SD), percentages, or medians (25th, 75th percentiles). Box-Cox transformation was applied to normalize the data before multifactorial analysis. Multivariate analysis included PCA and PLS-DA, with model fit assessed by R^2 and Q^2. Differential lipid metabolites were identified based on $q<0.05$, variable importance in the projection (VIP)>1, and fold change (FC)>1.2. Receiver operating characteristic (ROC) curves evaluated the sensitivity, specificity, and the area under the curve (AUC) of these metabolites in distinguishing groups. Spearman's rank correlation was used to test correlations, and 10-fold cross-validation was performed to assess model generalization. Statistical significance was set at $q<0.05$. To further investigate these differential metabolites, differential phospholipid pathway analysis was performed using MetaboAnalyst 6.0 (McGill University, Montreal, Canada).

RESULTS

Characteristics of Subjects

A total of 217 all-male subjects were included in the study: 62 with pneumoconiosis (PN group), 105 dust-exposed workers (EX group), and 50 healthy individuals (HT group). There were no significant differences in age, BMI, smoking status, alcohol consumption, or chronic disease prevalence across the three groups; however, the PN group had a significantly longer dust exposure duration than the EX group. Lung function tests were conducted on the PN and EX groups, with no significant differences observed (Table 1). After removing phospholipids with >30% missing values, the quantitative values for each group are listed in Table 2. In univariate analysis, significant differences in phospholipids were identified between the PN and HT groups, except for Lyso-PC (18:0), PC (14:0), and PI (16:0). Aside from PC (16:0, 18:0, 18:0/18:1) and PE (16:0,18:0), other phospholipids showed significant differences between the EX and HT groups. Excluding Lyso-PC (18:1,18:0), PE (18:0,18:0/18:1), PS (18:1), and PG (18:0/18:1), phospholipids displayed significant differences between the PN and EX groups.

Changes in Serum Phospholipids

A total of 22 phospholipids were quantified. After removing data with > 30% missing values, 18

TABLE 1. Characteristics of subjects.

Variable	PN (*n*=62)	EX (*n*=105)	HT (*n*=50)	*P*
Male (%)	100	100	100	1.000
Age (years)	45.03±3.30	45.16±3.14	46.64±6.66	0.084
BMI (kg/m^2)	24.01±2.70	23.62±2.13	24.16±2.62	0.371
Duration of exposure (years)	10.00 (7.00,12.25)	5.81 (4.47,7.21)	–	<0.001
Smoking (yes, %)	26 (41.9)	48 (45.7)	25 (50.0)	0.695
Drinking (yes, %)	40 (64.5)	66 (62.9)	34 (68.0)	0.822
Chronic disease (yes, %)	11 (17.7)	10 (9.5)	6 (12.0)	0.297
FEV1 (predicted %)	91±11.51	93.22±12.37	–	0.595
FEV1/FVC (%)	88.32±6.79	87.00±7.11	–	0.560
MMEF (L/S)	85.32±24.42	82.35±21.91	–	0.650
MEF75% (predicted %)	73.05±22.55	69.73±21.55	–	0.445
MEF50% (predicted %)	76.92±22.69	75.80±20.49	–	0.839
MEF25% (predicted %)	85.23±31.71	81.25±27.83	–	0.554

Note: "–" Lung function tests were not conducted for the HT group; "predicted" The predicted value in lung function testing; "±" The range of standard deviation.
Abbreviation: PN=patients with pneumoconiosis (PN group); EX=dust-exposed workers (EX group); HT=healthy individuals (HT group); BMI=body mass index; FEV1=forced expiratory volume in one second; FEV1/FVC=ratio of forced expiratory volume in one second to forced vital capacity; MMEF=maximum mid-expiratory flow; MEF75%=maximum expiratory flow at 75% of vital capacity; MEF50%=maximum expiratory flow at 50% of vital capacity; MEF25%=maximum expiratory flow at 25% of vital capacity.

TABLE 2. Quantitative values of phospholipids in each group [median (25th, 75th percentile) mg/L].

Phospholipid	PN	EX	HT
Lyso-PC (16:0)	54.324 (45.654, 64.642)*†	32.926 (27.371, 40.985)§	62.401 (55.161, 71.883)
Lyso-PC (18:1)	6.979 (4.665, 8.276)†	6.108 (4.065, 8.273)§	4.497 (3.439, 7.125)
Lyso-PC (18:0)	22.725 (14.433, 47.347)*	31.006 (24.933, 31.791)§	22.085 (17.760, 25.959)
PC (14:0)	0.058 (0.028, 0.090)*	0.106 (0.060, 0.191)§	0.051 (0.031, 0.055)
PC (16:0)	6.576 (5.679, 7.637)*†	3.856 (3.290, 4.687)	3.950 (3.399, 5.091)
PC (18:0)	0.989 (0.802, 1.203)*†	0.686 (0.596, 0.934)	0.630 (0.487, 0.864)
PC (16:0/18:1)	34.978 (28.596,42.964)*†	15.347 (12.679, 19.452)§	19.362 (16.214, 22.895)
PC (18:0/18:1)	23.470 (13.399, 38.674)*†	33.208 (26.150, 46.561)	35.626 (26.832, 44.475)
PE (16:0)	0.012 (0.005, 0.018)*†	0.019 (0.015, 0.027)	0.024 (0.017, 0.031)
PE (18:0)	0.579 (0.449, 0.750)†	0.516 (0.361, 0.073)	0.448 (0.183, 0.749)
PE (18:0/18:1)	1.616 (1.167, 2.290)†	1.393 (0.980, 2.102)§	1.010 (0.723, 1.943)
PI (16:0)	0.063 (0.042, 0.084)*	0.120 (0.040, 0.175)§	0.027 (0.021, 0.041)
PI (16:0/18:1)	0.746 (0.513, 1.109)*†	0.319 (0.218, 0.432)§	0.206 (0.144, 0.266)
Lyso-PS (18:0)	0.055 (0.038, 0.109)*†	0.151 (0.062, 0.264)§	0.196 (0.120, 0.437)
PS (16:0)	0.008 (0.005, 0.011)*†	0.012 (0.008, 0.018)§	0.008 (0.004, 0.011)
PS (18:1)	0.030 (0.024, 0.037)†	0.027 (0.016, 0.046)§	0.014 (0.007, 0.027)
PG (16:0)	0.137 (0.114, 0.170)*†	0.067 (0.046, 0.085)§	0.028 (0.023, 0.035)
PG (18:0/18:1)	0.159 (0.121, 0.194)†	0.148 (0.115, 0.179)§	0.066 (0.052, 0.093)

Abbreviation: PN=patients with pneumoconiosis (PN group); EX=dust-exposed workers (EX group); HT=healthy individuals (HT group); Lyso-PC=lyso-phosphatidylcholine; PC=phosphatidylcholine; PE=phosphatidylethanolamine; PI=phosphatidylinositol; Lyso-PS=lyso-phosphatidylserine; PS=phosphatidylserine; PG=phosphatidylglycerol.
* q<0.05 between PN and EX group.
† q<0.05 between PN and HT group.
§ q<0.05 between EX and HT group.

phospholipids were analyzed. The remaining missing values were imputed using the detection limit divided by √2. Principal component analysis (PCA) was used to evaluate significant overall differences in phospholipids among the three groups (Figure 1AB). PCA successfully separated the PN group from the other two groups but did not fully distinguish them. Partial least squares discriminant analysis (PLS-DA) revealed a distinct separation of serum phospholipid metabolism profiles between the PN and HT groups (Figure 1C– with R^2Y=0.924, Q^2Y=0.915) and between the PN and EX groups (Figure 1E–F, with R^2Y=0.922, Q^2Y=0.902). Scatter plots of R^2Y and Q^2Y values for the actual and simulated models after random permutation (Supplementary Figure S1, available at https://weekly.chinacdc.cn/) demonstrated no overfitting.

Differential Metabolite Screening

In this study, we screened for metabolite differences between groups using univariate and multivariate statistical analyses (Supplementary Tables S1–S2, available at https://weekly.chinacdc.cn/). Based on a q<0.05, FC>1.2, and VIP>1, we identified five phospholipids that differed significantly between the EX and HT groups: lyso-PC (16:0), PC (14:0), PS (18:1), PG (16:0), and PG (18:0/18:1). These were generally higher in the EX group than in the HT group.

Furthermore, eight distinct phospholipids were identified when comparing the PN and HT groups, and their potential to discriminate between CWP patients and healthy individuals was verified using receiver operating characteristic (ROC) curve analysis. These phospholipids included PC (16:0), PC (16:0/18:1), PI (16:0/18:1), Lyso-PS (18:0), PS (18:1), PG (16:0), and PG (18:0/18:1), with AUCs and sensitivities greater than 0.7. Violin plots illustrated the distribution of these potential biomarker levels by group. Except for Lyso-PS (18:0), which showed a decrease, the levels of the other differential phospholipids all exhibited elevation in the PN group (Figure 1G, 1I).

To differentiate patients with pneumoconiosis from exposed individuals, ROC curves were analyzed for seven differential phospholipids after filtering with the established criteria. Among these, Lyso-PC (16:0), PC (16:0), PC (16:0/18:1), PI (16:0/18:1), and PG (16:0) exhibited good results. All differential phospholipids were consistently higher in the pneumoconiosis group than in the exposed group (Figure 1H, 1J).

Cross-Validation for Potential Biomarkers

To seek clues for early diagnostic biomarkers, it is necessary to distinguish phospholipid alterations occurring during the dust-exposure period from those present when the criteria for pneumoconiosis are met. In comparing the PN with the HT and EX groups, PC (16:0), PC (16:0/18:1), PI (16:0/18:1), and PG (16:0) were common differential metabolites with a consistent direction of regulation (Figure 2A). As this study is a preliminary investigation, we developed a support vector machine (SVM) model between the PN and EX groups to enhance discriminative power, selecting the four overlapping phospholipids as potential biomarkers. We assessed the model's generalization ability using ten-fold cross-validation, randomly dividing the subjects into 10 groups, with nine serving as validation sets and one as the training set. As shown in Figure 2B, the model demonstrated highly satisfactory efficacy metrics. The mean values for AUC, sensitivity, specificity, and accuracy were 0.956, 0.934, 0.783, and 0.911, respectively. This combination is more effective at distinguishing between groups than most individual phospholipids.

Enrichment Analysis of Differential Phospholipids and Correlation Analysis with Lung Function.

As shown in Figure 2C, four pathways were identified, with the majority enriched in glycerophosphocoline metabolism. Figure 2D illustrates that only PC (16:0) was positively correlated with MEF25% (L/s), although the correlation coefficients were modest.

DISCUSSION

In this study, we applied our team's UPLC-MS/MS phospholipid-targeted quantification method to investigate CWP. Unlike previous untargeted metabolomics studies, this targeted approach provided precise phospholipid quantification, offering specific insights into CWP-associated metabolic changes. Our findings showed that coal dust exposure significantly altered serum phospholipids, with variations effectively distinguishing patients with CWP. PC, PI, Lyso-PS, PS, and PG differentiated the PN and HT groups, while Lyso-PC, PC, PI, and PG distinguished the PN and EX groups. A model including PC (16:0), PC (16:0/18:1), PI (16:0/18:1), and PG (16:0) demonstrated strong discriminatory power between

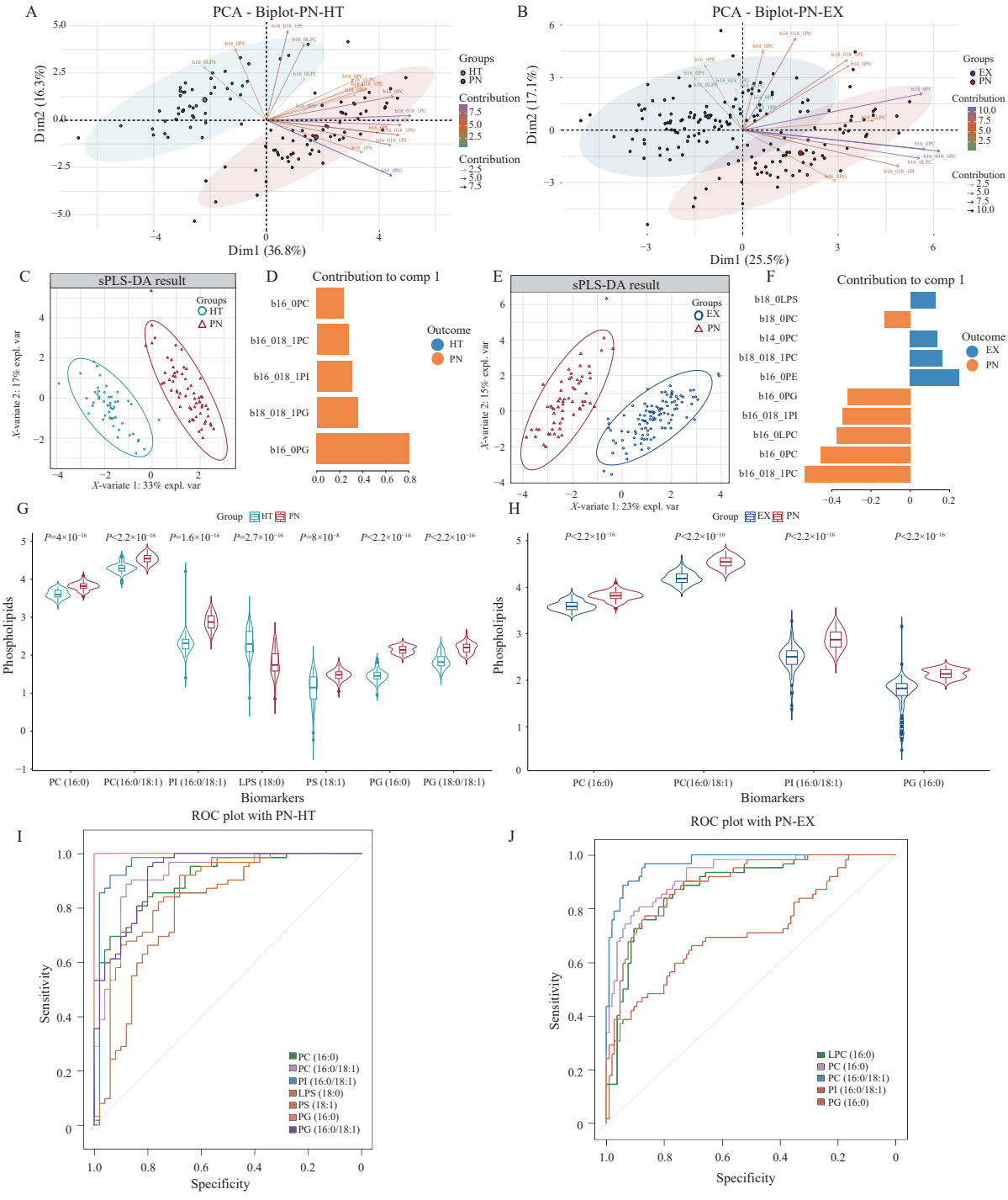

FIGURE 1. The results of univariate and multivariate analyses between two groups. (A) PCA mode between the PN and HT groups. (B) PCA model between the PN and EX groups. (C) PLS-DA results for the PN and HT groups, with R^2Y=0.924, Q^2Y=0.915. (D) Principal component contribution to differentiate between PN and HT group. (E) PLS-DA results for the PN and EX group, with R^2Y=0.922, Q^2Y=0.902. (F) Principal component contribution to differentiate between PN and EX group. (G) Violin plot showing differential phospholipids in the PN and HT groups. (H) Violin plot showing differential phospholipids in the PN and EX groups. (I) ROC curve for differential phospholipids in the PN and HT groups. (J) ROC curve for differential phospholipids in the PN and EX groups.

Abbreviation: PN=patients with pneumoconiosis (PN group); EX=dust-exposed workers (EX group); HT=healthy individuals (HT group); PC=phosphatidylcholine; LPC=lyso-phosphatidylcholine; PI=phosphatidylinositol; LPS=lyso-phosphatidylserine; PS=phosphatidylserine; PG=phosphatidylglycerol; CWP=coal worker's pneumoconiosis; PCA=principal component analysis; ROC=receiver operating characteristic.

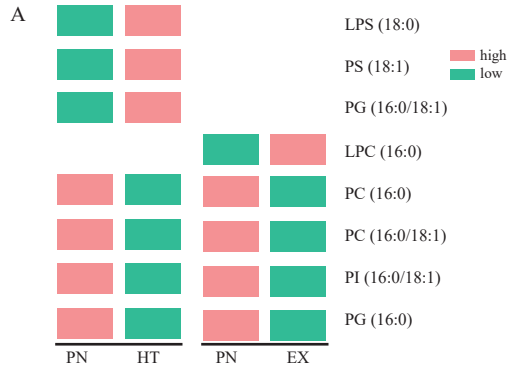

B

Fold	AUC	Sensitivity	Specificity	Accuracy
1	0.985	0.909	1.000	0.941
2	0.909	1.000	0.500	0.824
3	0.971	0.800	1.000	0.889
4	0.950	1.000	0.833	0.938
5	0.985	1.000	0.667	0.824
6	0.967	1.000	0.500	0.938
7	1.000	1.000	0.833	1.000
8	0.894	0.727	0.833	1.000
9	0.900	0.900	1.000	0.941
10	1.000	1.000	0.667	0.813
Average	0.956	0.934	0.783	0.911

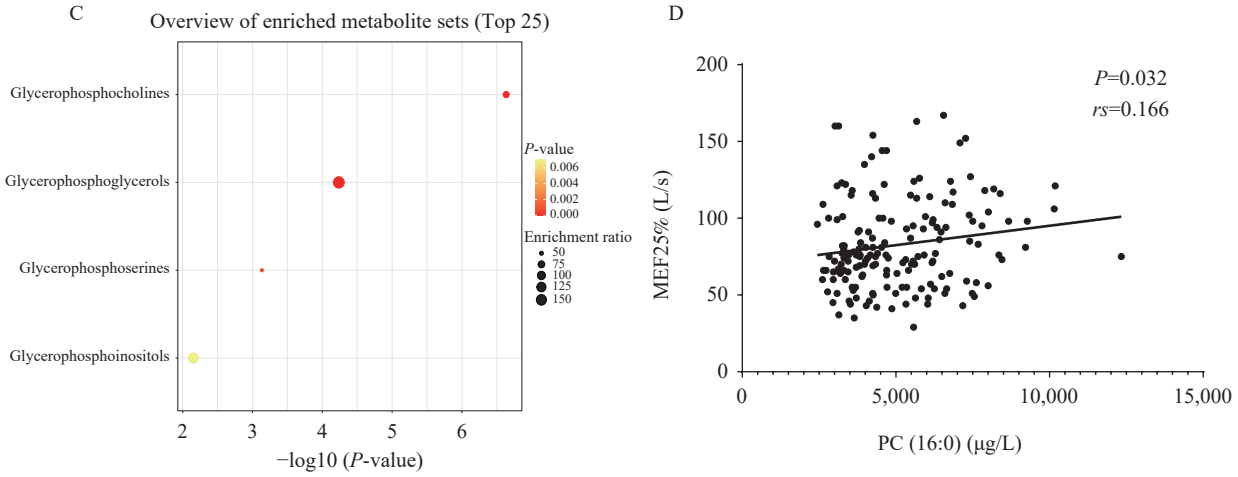

FIGURE 2. Validation of differential phospholipids as potential biomarkers for pneumoconiosis. (A) Regulation of overlapping phospholipids. (B) Ten-fold cross-validation for potential biomarkers. (C) Pathway enrichment analysis of differential phospholipids. (D) Scatter plot illustrating the correlation between PC (16:0) and pulmonary function.
Abbreviation: PN=patients with pneumoconiosis (PN group); EX=dust-exposed workers (EX group); HT=healthy individuals (HT group); LPS=lyso-phosphatidylserine; PS=phosphatidylserine; LPC=lyso-phosphatidylcholine; PC=phosphatidylcholine; PI=phosphatidylinositol; PG=phosphatidylglycerol; AUC=area under the curve; MEF25%=maximum expiratory flow at 25% of vital capacity.

coal dust-exposed individuals and patients with CWP, suggesting these lipids as potential early diagnostic biomarkers and providing a valuable reference for auxiliary diagnosis. These phospholipids were primarily involved in glycerophospholipid metabolism and could serve as reliable biomarkers for pneumoconiosis if their biological roles are confirmed.

Lipids are a significant component of lung surfactant, and phospholipids, particularly PC, are the major constituents (*8*–*9*). Research has demonstrated a pivotal role for PCs in the inflammatory response. Studies, including our own, have revealed an association between elevated PC levels and coal dust exposure. Phospholipase A2 hydrolyzes PC to produce lyso-PC, which plays an important role in the onset and progression of inflammation and is potentially associated with pulmonary fibrosis. Lyso-PC metabolism via phospholipase A2 (*10*) or autotaxin (*11*) in bronchial epithelial cells or macrophages is implicated in pulmonary fibrosis. These findings suggest that alterations in PC and lyso-PC metabolism may contribute to lung fibrosis development.

PG has been implicated in the anti-inflammatory process. Consistent with other studies (*12*), PG levels were elevated at earlier time points and remained elevated in comparisons between pneumoconiosis patients and dust-exposed individuals. Therefore, we considered the potential for PG to serve as an early biomarker. PI-associated endoplasmic reticulum stress (*13*) and the downstream PIP3-AKT pathway (*14*) have also been implicated in pulmonary fibrosis.

Our findings indicate that the identified potential biomarkers are primarily associated with the glycerophosphorylcholine (GPC) pathway. GPC binding to aldehydes induces macrophage apoptosis, leading to airway damage and inflammation (*15*). However, no published studies have investigated GPC metabolism in CWP. Therefore, further research is

warranted.

This study has some limitations. First, the sample size for each group was relatively small, and no validation set was used for sample verification. Future studies will expand the sample size to verify these findings. Second, this study did not consider the potential impact of dietary habits on metabolic profiles. However, because all participants reside in the same region and are predominantly local, their dietary and lifestyle habits are likely very similar. Third, the range of phospholipids examined in this study was limited. Expanding the number of targeted phospholipid species in future studies would broaden the scope and further screen for potential lipid biomarkers for pneumoconiosis. Furthermore, additional functional validation studies on these phospholipids would help identify biomarkers for coal worker's pneumoconiosis.

doi: 10.46234/ccdcw2024.279

[#] Corresponding authors: Chunguang Ding, ding_chg@163.com; Yiwei Shi, shiyw@sxmu.edu.cn.

[1] Guangdong Pharmaceutical University, Guangzhou City, Guangdong Province, China; [2] National Center for Occupational Safety and Health, NHC, Beijing, China; [3] NHC Key Laboratory for Engineering Control of Dust Hazard, Beijing, China; [4] National Institute for Occupational Health and Poison Control, Chinese Center for Disease Control and Prevention, Beijing, China; [5] NHC Key Laboratory of Pneumoconiosis, MOE Key Laboratory of Coal Environmental Pathogenicity and Prevention, Shanxi Key Laboratory of Respiratory Diseases, The First Hospital of Shanxi Medical University, Taiyuan City, Shanxi Province, China.

Submitted: January 08, 2024
Accepted: December 17, 2024
Issued: December 27, 2024

REFERENCES

1. Chu SG, Villalba JA, Liang XL, Xiong K, Tsoyi K, Ith B, et al. Palmitic acid-rich high-fat diet exacerbates experimental pulmonary fibrosis by modulating endoplasmic reticulum stress. Am J Respir Cell Mol Biol 2019;61(6):737 – 46. https://doi.org/10.1165/rcmb.2018-0324OC.
2. Suryadevara V, Ramchandran R, Kamp DW, Natarajan V. Lipid mediators regulate pulmonary fibrosis: potential mechanisms and signaling pathways. Int J Mol Sci 2020;21(12):4257. https://doi.org/10.3390/ijms21124257.
3. Burgy O, Loriod S, Beltramo G, Bonniaud P. Extracellular lipids in the lung and their role in pulmonary fibrosis. Cells 2022;11(7):1209. https://doi.org/10.3390/cells11071209.
4. Oikonomou N, Mouratis MA, Tzouvelekis A, Kaffe E, Valavanis C, Vilaras G, et al. Pulmonary autotaxin expression contributes to the pathogenesis of pulmonary fibrosis. Am J Respir Cell Mol Biol 2012;47(5):566 – 74. https://doi.org/10.1165/rcmb.2012-0004OC.
5. Peng FD, Dai J, Qian QJ, Cao XF, Wang LF, Zhu M, et al. Serum metabolic profiling of coal worker's pneumoconiosis using untargeted lipidomics. Environ Sci Pollut Res Int 2022;29(56):85444 – 53. https://doi.org/10.1007/s11356-022-21905-4.
6. Ma RM, Fan YL, Huang XX, Wang JW, Li S, Wang YY, et al. Lipid dysregulation associated with progression of silica-induced pulmonary fibrosis. Toxicol Sci 2023;191(2):296 – 307. https://doi.org/10.1093/toxsci/kfac124.
7. Wang WR, Peng FD, Ding CG, Li T, Wang HQ. An analysis of targeted serum lipidomics in patients with pneumoconiosis – China, 2022. China CDC Wkly 2023;5(38):849 – 55. https://doi.org/10.46234/ccdcw2023.161.
8. Agudelo CW, Samaha G, Garcia-Arcos I. Alveolar lipids in pulmonary disease. A review. Lipids Health Dis 2020;19(1):122. https://doi.org/10.1186/s12944-020-01278-8.
9. Agassandian M, Mallampalli RK. Surfactant phospholipid metabolism. Biochim Biophys Acta 2013;1831(3):612 – 25. https://doi.org/10.1016/j.bbalip.2012.09.010.
10. Deng XD, Hao CF, Li YP, Guo YH, Si HF, He J, et al. Lysophosphatidylcholine acyltransferase 1 alleviates silica-induced pulmonary fibrosis by modulating lipid metabolism. Biomed Pharmacother 2022;155:113638. https://doi.org/10.1016/j.biopha.2022.113638.
11. Magkrioti C, Galaris A, Kanellopoulou P, Stylianaki EA, Kaffe E, Aidinis V. Autotaxin and chronic inflammatory diseases. J Autoimmun 2019;104:102327. https://doi.org/10.1016/j.jaut.2019.102327.
12. Saito K, Tanaka N, Ikari J, Suzuki M, Anazawa R, Abe M, et al. Comprehensive lipid profiling of bleomycin-induced lung injury. Appl Toxicol 2019;39(4):658 – 71. https://doi.org/10.1002/jat.3758.
13. Hsu HS, Liu CC, Lin JH, Hsu TW, Hsu JW, Su K, et al. Involvement of ER stress, PI3K/AKT activation, and lung fibroblast proliferation in bleomycin-induced pulmonary fibrosis. Sci Rep 2017;7(1):14272. https://doi.org/10.1038/s41598-017-14612-5.
14. Zhang H, Zhang SQ, Wang Y, Zhang CL. Preliminary study of exon sequence in pneumoconiosis using high-throughput and intervention of EGFR-TKIs on silicosis rats. Chin J Ind Hyg Occup Dis 2019;37(6):408 – 15. https://doi.org/10.3760/cma.j.issn.1001-9391.2019.06.002.
15. Uhlson C, Harrison K, Allen CB, Ahmad S, White CW, Murphy RC. Oxidized phospholipids derived from ozone-treated lung surfactant extract reduce macrophage and epithelial cell viability. Chem Res Toxicol 2002;15(7):896 – 906. https://doi.org/10.1021/tx010183i.

SUPPLEMENTARY MATERIAL

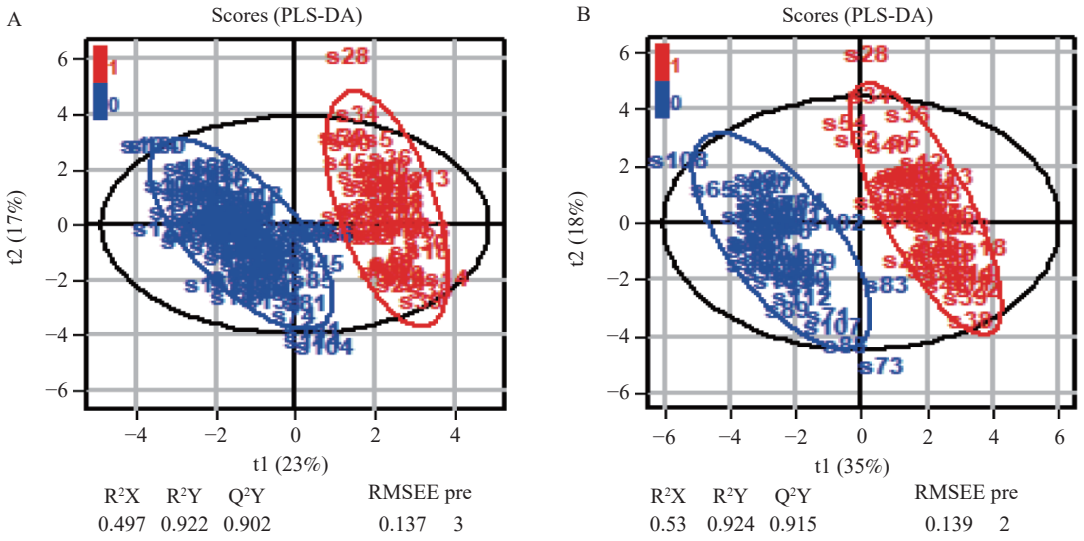

SUPPLEMENTARY FIGURE S1. Permutation tests of PLS-DA models. (A) Scores plot for PN and EX group; (B) Scores plot for PN and HT groups.
Abbreviation: PLS-DA=partial least squares discriminant analysis; PN=patients with pneumoconiosis (PN group); EX=dust-exposed workers (EX group); HT=healthyindividuals (HT group).

SUPPLEMENTARY TABLE S1. Univariate and multivariate statistical results for PN and HT groups.

Phospholipid	VIP	FC	q
Lyso-PC (16:0)	0.692	1.14	<0.001
Lyso-PC (18:1)	0.635	1.55	<0.001
Lyso-PC (18:0)	0.226	1.03	0.446
PC (14:0)	0.540	1.13	0.057
PC (16:0)	1.248	1.66	<0.001
PC (18:0)	0.939	1.57	<0.001
PC (16:0/18:1)	1.284	1.81	<0.001
PC (18:0/18:1)	1.060	1.52	<0.001
PE (16:0)	0.967	1.92	<0.001
PE (18:0)	0.595	1.29	0.011
PE (18:0/18:1)	0.666	1.60	0.012
PI (16:0)	1.046	2.38	0.056
PI (16:0/18:1)	1.298	3.63	<0.001
Lyso-PS (18:0)	1.080	3.57	<0.001
PS (16:0)	0.269	1.07	0.047
PS (18:1)	1.025	2.17	0.002
PG (16:0)	1.721	4.83	<0.001
PG (18:0/18:1)	1.341	2.41	<0.001

Note: Student's t-test (data normally distributed)/ Mann-Whitney U-test (data non-normally distributed) for continuous variables and Pearson's χ^2 test for categorical variables was used to evaluate the differences between groups. The p-values were adjusted for FDR using the Benjamini-Hochberg method and expressed as q-values. VIP value were derived from PLS-DA analysis. FC value (obtained by div iding the median of the larger group by that of the smaller group).
Abbreviation: VIP=variable importance in projection; FC=fold change; Lyso-PC=lyso-phosphatidylcholine; PC=phosphatidylcholine; PE=phosphatidylethanolamine; PI=phosphatidylinositol; Lyso-PS=lyso-phosphatidylserine; PS=phosphatidylserine; PG=phosphatidylglycerol.

SUPPLEMENTARY TABLE S2. Univariate and multivariate statistical results for PN and EX groups.

Phospholipid	VIP	FC	q
Lyso-PC (16:0)	1.420	1.65	<0.001
Lyso-PC (18:1)	0.792	1.14	0.232
Lyso-PC (18:0)	0.367	1.36	0.186
PC (14:0)	0.946	1.81	<0.001
PC (16:0)	1.583	1.71	<0.001
PC (18:0)	0.931	1.44	<0.001
PC (16:0/18:1)	1.764	2.28	<0.001
PC (18:0/18:1)	1.093	1.41	<0.001
PE (16:0)	1.141	1.55	<0.001
PE (18:0)	0.368	1.12	0.136
PE (18:0/18:1)	0.388	1.16	0.232
PI (16:0)	0.662	1.90	<0.001
PI (16:0/18:1)	1.334	2.34	<0.001
Lyso-PS (18:0)	0.857	2.75	<0.001
PS (16:0)	0.617	1.43	<0.001
PS (18:1)	0.093	1.12	0.893
PG (16:0)	1.284	2.04	<0.001
PG (18:0/18:1)	0.259	1.07	0.889

Note: Student's t-test (data normally distributed)/ Mann-Whitney U-test (data non-normally distributed) for continuous variables and Pearson's χ^2 test for categorical variables were used to evaluate the differences between groups. The *P*-values were adjusted for FDR using the Benjamini-Hochberg method and expressed as q-values. VIP values were derived from PLS-DA analysis. FC values (calculated by dividing the median of the larger group by that of the smaller group).

Abbreviation: VIP=variable importance in projection; FC=fold change; Lyso-PC=lyso-phosphatidylcholine; PC=phosphatidylcholine; PE=phosphatidylethanolamine; PI=phosphatidylinositol; Lyso-PS=lyso-phosphatidylserine; PS=phosphatidylserine; PG= phosphatidylglycerol.

Recollection

Analysis of Mortality and Life Expectancy Determinants Among 5,791 Deceased Pneumoconiosis Patients — Jiangsu Province, China, 2011–2023

Hangju Zhu[1,2,&]; Lang Zhou[3,&]; Jinyi Zhou[4]; Lei Han[3,#]; Ming Wu[1,4,#]

ABSTRACT

Pneumoconiosis is the occupational disease with the highest proportion in China. This study conducted a retrospective analysis of 5,791 deceased pneumoconiosis patients. In this study, males comprised 93.02% of cases, with primary affected industries being mining (58.47%), manufacturing (20.55%), and public management (16.42%). Silicosis (69.42%) and coal worker's pneumoconiosis (20.57%) were the predominant diagnoses. Most patients (66.47%) were diagnosed at stage one. Significant differences were observed in both diagnosis age and post-diagnosis survival time across disease stages (P<0.05). The proportion of patients who died directly from lung infections was the highest (37.32%). The primary underlying causes of death in pneumoconiosis patients include pulmonary infections, cardiovascular and cerebrovascular diseases, and digestive tract and lung tumors. Life expectancy for patients aged 30–35 years was 15.83 years. After excluding the effects of pulmonary infections, cardiovascular diseases, digestive tract tumors, and lung tumors, life expectancy increased by 3.75, 1.11, 1.31, and 0.63 years, respectively. Pneumoconiosis patients with concurrent lung tumors showed a 7.797-fold increased mortality risk, while pulmonary infections elevated mortality risk by 3.030-fold. Management strategies for pneumoconiosis should emphasize both primary disease treatment and comprehensive care for complications, particularly pulmonary infections, cardiovascular diseases, and malignancies. This integrated approach could extend survival time and enhance quality of life for affected patients.

Pneumoconiosis frequently leads to pulmonary fibrosis and compromised lung immunity in affected individuals. Given the irreversible nature of pulmonary fibrosis, pneumoconiosis remains a preventable but currently incurable occupational disease (*1*). The reduced lung immunity in these patients often precipitates multiple complications, including emphysema, tuberculosis, and lung cancer (*2*). These comorbidities significantly complicate both the prevention and treatment of pneumoconiosis, with existing research demonstrating elevated mortality rates among pneumoconiosis patients with concurrent health conditions (*3*).

This study presents a comprehensive medical analysis of 5,791 deceased pneumoconiosis patients. Through detailed examination of the fundamental causes of death, This study aims to elucidate the primary mortality factors among these patients, evaluate the impact of various causes of death on their life expectancy, and provide evidence-based insights to inform future prevention and treatment strategies for pneumoconiosis.

METHODS

Study Population

This study analyzed data from the Jiangsu Province pneumoconiosis follow-up online reporting system. The study cohort comprised 5,791 deceased patients with complete follow-up information recorded between January 1, 2011, and December 31, 2023. The cohort included 5,387 male and 404 female patients, with ages at death ranging from 32 to 101 years (mean: 76.63±8.98 years). Two patients with silicosis and other types of pneumoconiosis, respectively, died at ages exceeding 100 years. Data from 15,838 surviving patients were used to construct a simplified life table for pneumoconiosis patients in Jiangsu Province.

Statistical Analysis

Data collection encompassed patients' occupational industry, pneumoconiosis type, disease stage at

diagnosis, primary cause of death, age at diagnosis, and post-diagnosis survival time. Statistical analyses were performed using SPSS (version 23.0, IBM, Chicago, USA) and R software (version 4.4.1, Ross Ihaka, Auckland, New Zealand). One-way ANOVA (Analysis of Variance) was employed to compare intergroup means, while the Cox proportional hazards regression model was used for multivariate survival analysis. Statistical significance was set at $P<0.05$.

The primary cause of death was classified according to the International Classification of Diseases, Injuries, and Causes of Death (ICD) (*4*). This was defined as the initial disease or injury that initiated the sequence of pathological events leading directly to death, or the accident or violent event causing fatal injury. Causes of death were categorized as: lung infection, cardiovascular and cerebrovascular diseases, gastrointestinal tumors, lung tumors, trauma and other accidents, other tumors, diabetes, Parkinson's disease, and other diseases (including sudden death, massive hemorrhage from gastrointestinal ulcer, and acute and chronic organ failure).

Occupational industries were classified according to the GB/T 4754-2017 Classification of National Economic Industries. Using follow-up data from 15,838 surviving patients in the online reporting system as of December 2023, we constructed both a simplified life table and a cause-specific life table. These analyses were conducted to evaluate the life expectancy of pneumoconiosis patients and quantify the impact of different causes of death on their life expectancy (*5*).

RESULTS

Patient Characteristics

Among the 5,791 pneumoconiosis patients, males comprised 93.02% of the cohort, significantly outnumbering females (6.98%). The occupational distribution revealed that mining (58.47%), manufacturing (20.55%), and public management, social security, and social organizations (16.42%) were the predominant sectors, collectively accounting for 95.44% of cases. Silicosis (69.42%) and coal worker's pneumoconiosis (20.57%) were the most prevalent types, representing 89.99% of all cases. The majority of patients (66.47%) were diagnosed with stage one pneumoconiosis (Table 1).

Survival Time

The average age at diagnosis for the 5,791 deceased patients with pneumoconiosis was 58.52±11.38 years, with an average post-diagnosis survival time of 18.12±11.21 years. Patients diagnosed with stage I pneumoconiosis exhibited a higher mean age at diagnosis compared to those with stages II and III. Conversely, stage II patients demonstrated longer post-diagnosis survival times than those with stages I and III. Statistical analysis revealed significant differences in both diagnostic age and post-diagnosis survival time across all pneumoconiosis stages ($P<0.05$) (Table 2).

Cause of Death

Analysis of the 5,791 deaths reveals four predominant causes of mortality: pulmonary infections (37.32%), cardiovascular and cerebrovascular diseases (22.71%), gastrointestinal tumors (14.57%), and lung tumors (11.97%). For patients with stage I and II pneumoconiosis, the mortality pattern follows this same hierarchical order. However, in stage III pneumoconiosis patients, while pulmonary infections and cardiovascular and cerebrovascular diseases remain the leading causes, lung tumors supersede gastrointestinal tumors as the third most common cause of death. These findings demonstrate that pulmonary infections, cardiovascular and cerebrovascular diseases, and tumors of the gastrointestinal tract and lungs constitute the principal causes of mortality across all stages of pneumoconiosis (Table 3).

Life Expectancy of Pneumoconiosis Patients

Using 2023 follow-up data from 15,838 surviving pneumoconiosis patients in Jiangsu Province, we constructed a simplified life table. Based on age-specific mortality probabilities and assuming a cohort of 10,000 pneumoconiosis patients aged 30 to <35 years, we calculated the number of surviving patients and expected life expectancy for each age group. The analysis projects an average life expectancy of 15.83 years for these pneumoconiosis patients (Table 4).

The Impact of Different Causes of Death on Life Expectancy

Table 5 presents a comparative analysis of life expectancy using multiple cause-specific life tables. The baseline life table for pneumoconiosis patients was

TABLE 1. Patient characteristics of 5,791 deceased pneumoconiosis patients.

Factor	Number	Percentage (%)
Gender		
Male	5,387	93.02
Female	404	6.98
Industry		
Industry	3,386	58.47
Manufacturing industry	1,190	20.55
Public administration, social security and social organizations	951	16.42
Electricity, heat, gas and water production and supply	106	1.83
Construction	79	1.36
Wholesale and retail	22	0.38
Residential services, repair and other services	17	0.29
Agriculture, forestry, animal husbandry and fishery	14	0.24
Water conservancy, environment and public facilities Management	10	0.17
Culture, sports and entertainment	5	0.09
Leasing and business services	4	0.07
Health and social work	3	0.05
Education	2	0.03
Real estate	1	0.02
Scientific research and technology services	1	0.02
Types of pneumoconiosis		
Silicosis	4,020	69.42
Coal worker's pneumoconiosis	1,191	20.57
Founder pneumoconiosis	146	2.52
Asbestosis	121	2.09
Cement pneumoconiosis	110	1.90
Kaolin pneumoconiosis	76	1.31
Other pneumoconiosis diseases	56	0.97
Welder's pneumoconiosis	47	0.81
Carbon black pneumoconiosis	7	0.12
Talcosis	7	0.12
Aluminosis	6	0.10
Graphite pneumoconiosis	2	0.03
Mica pneumoconiosis	2	0.03
Diagnosis period		
Phase I pneumoconiosis	3,849	66.47
Phase II pneumoconiosis	1,401	24.19
Phase III pneumoconiosis	541	9.34

TABLE 2. Survival time of 5,791 deceased pneumoconiosis patients.

Diagnosis period	Average age at diagnosis (years)		Average survival time after diagnosis (years)	
Phase I pneumoconiosis	58.88±11.21	F=6.847 P<0.05	17.72±10.93	F=19.479 P<0.05
Phase II pneumoconiosis	58.00±11.61		19.68±11.46	
Phase III pneumoconiosis	57.24±11.87		16.86±12.45	
Amount to	58.52±11.38		18.12±11.21	

TABLE 3. Cause of death of 5,791 deceased pneumoconiosis patients.

underlying cause of death	Phase I pneumoconiosis			Phase II pneumoconiosis			Phase III pneumoconiosis			Amount to		
	Number	Percentage (%)	Rank order of causes of death	Number	Percentage (%)	Rank order of causes of death	Number	Percentage (%)	Rank order of causes of death	Number	Percentage (%)	Rank order of causes of death
Pulmonary infection	1,223	31.77	1	591	42.18	1	347	64.14	1	2,161	37.32	1
Cardiovascular and cerebrovascular diseases	970	25.20	2	285	20.34	2	60	11.09	2	1,315	22.71	2
Gastrointestinal tumors	606	15.74	3	195	13.92	3	43	7.95	4	844	14.57	3
Lung tumors	496	12.89	4	146	10.42	4	51	9.43	3	693	11.97	4
Other diseases	181	4.70	5	56	4.00	5	14	2.59	6	251	4.33	5
Accidents such as trauma	148	3.85	6	52	3.71	6	15	2.77	5	215	3.71	6
Other tumors	121	3.14	7	44	3.14	7	8	1.48	7	173	2.99	7
Diabetes	75	1.95	8	27	1.93	8	2	0.37	8	104	1.80	8
Parkinson's disease	29	0.75	9	5	0.36	9	1	0.18	9	35	0.60	9

TABLE 4. Brief life table of follow-up patients with pneumoconiosis in Jiangsu Province in 2023.

Age group (years)	Number of observers	Actual number of deaths	Mortality	Probability of death	Number of survivors	Death toll	Survival years	Total survival years	Life expectancy
30–34	14	1	0.071,4	0.303,0	10,000	3,030	42,424	158,327	15.83
35–39	65	2	0.030,8	0.142,9	6,970	996	32,359	115,903	16.63
40–44	140	5	0.035,7	0.163,9	5,974	979	27,422	83,544	13.98
45–49	329	20	0.060,8	0.263,9	4,995	1,318	21,679	56,122	11.24
50–54	789	36	0.045,6	0.204,8	3,677	753	16,502	34,443	9.37
55–59	1,141	140	0.122,7	0.469,5	2,924	1,373	11,188	17,941	6.14
60–64	1,372	316	0.230,3	0.730,8	1,551	1,134	4,922	6,754	4.35
65–69	3,183	741	0.232,8	0.735,8	418	307	1,320	1,832	4.39
70–74	5,357	1,012	0.188,9	0.641,6	110	71	375	512	4.64
75–79	4,263	1,143	0.268,1	0.802,6	40	32	118	137	3.47
80–84	2,856	1,223	0.428,2	1.034,1	8	8	19	19	2.44
≥85	2,120	1,152	0.543,4	1.000,0	0	0	0	0	0

Note: The probability of death in the age group ≥85 years old is 1.

TABLE 5. Brief current life table of causes of lung infection in 2023 follow-up patients with pneumoconiosis in Jiangsu Province.

Age group (years)	Number of observers	Total number of deaths from all causes	Deaths from pulmonary infections	Death rate due to lung infection	Probability of death	Survival Probability	Free from pulmonary infections					
							Survival Probability	Number of survivors	Death toll	Survival years	Total survival years	Life expectancy
30–34	14	1	0	1.000,0	0.303,0	0.697,0	0.697,0	10,000	3,030	42,424	216,620	21.66
35–39	65	2	2	0	0.142,9	0.857,1	1.000,0	6,970	0	34,848	174,196	24.99
40–44	140	5	5	0	0.163,9	0.836,1	1.000,0	6,970	0	34,848	139,347	19.99
45–49	329	20	10	0.500,0	0.263,9	0.736,1	0.858,0	6,970	990	32,374	104,499	14.99
50–54	789	36	17	0.527,8	0.204,8	0.795,2	0.886,1	5,980	681	28,197	72,125	12.06
55–59	1,141	140	60	0.571,4	0.469,5	0.530,5	0.696,1	5,299	1,610	22,468	43,928	8.29
60–64	1,372	316	100	0.683,5	0.730,8	0.269,2	0.407,8	3,689	2,184	12,982	21,460	5.82
65–69	3,183	741	206	0.722,0	0.735,8	0.264,2	0.382,5	1,504	929	5,199	8,478	5.64
70–74	5,357	1,012	272	0.731,2	0.641,6	0.358,4	0.472,3	575	304	2,118	3,279	5.70
75–79	4,263	1,143	413	0.638,7	0.802,6	0.197,4	0.354,8	272	175	920	1161	4.27
80–84	2,856	1,223	519	0.575,6	1.034,1	0	0	96	96	241	241	2.50
≥85	2,120	1,152	557	0.516,5	1.000,0	0	0	0	0	0	0	0

Note: The probability of death in the age group ≥ 85 years old is 1.

TABLE 6. The impact of different causes of death on life expectancy (years).

Age group (years)	Life expectancy for all causes of death	Life expectancy free from lung infections	Life expectancy free from cardiovascular and cerebrovascular diseases	Life expectancy free from digestive tract tumors	Life expectancy free from lung tumors	Life expectancy free from other diseases	Life expectancy free from trauma and accidents	Life expectancy free from other tumor	Life expectancy free from diabetes	Life expectancy free from Parkinson's disease
30–34	15.83	21.66	16.39	16.49	16.15	21.79	15.90	16.01	15.85	15.83
35–39	16.63	24.99	17.43	17.57	17.09	16.79	16.73	16.89	16.66	16.63
40–44	13.98	19.99	14.91	15.09	14.52	14.18	14.10	14.29	14.02	13.99
45–49	11.24	14.99	12.35	12.55	11.87	11.47	11.37	11.60	11.28	11.24
50–54	9.37	12.06	10.28	10.54	9.85	9.68	9.55	9.49	9.43	9.37
55–59	6.14	8.29	6.85	6.99	6.68	6.47	6.37	6.28	6.21	6.14
60–64	4.35	5.82	4.96	5.16	4.97	4.55	4.60	4.54	4.40	4.36
65–69	4.39	5.64	5.09	5.31	5.08	4.53	4.55	4.50	4.43	4.40
70–74	4.64	5.70	5.32	5.25	5.19	4.75	4.76	4.76	4.72	4.67
75–79	3.47	4.27	3.93	3.73	3.74	3.53	3.56	3.53	3.53	3.51
80–84	2.44	2.50	2.50	2.50	2.50	2.50	2.50	2.50	2.50	2.50
≥85	0	0	0	0	0	0	0	0	0	0

compared with life tables excluding specific causes of death, including pulmonary infections, cardiovascular and cerebrovascular diseases, gastrointestinal tumors, lung tumors, trauma and accidents, other tumors, diabetes, Parkinson's disease, and other conditions. The summarized findings are presented in Table 6. It was observed that the life expectancy of patients who succumbed to pulmonary infections was notably prolonged. Examination of Table 5 reveals extremely low or zero mortality rates were observed in the 35–45 year age group, which could introduce statistical bias, the analysis primarily focused on the 45–50 year age group. After excluding individual causes of death, the increases in life expectancy were: pulmonary infections (3.75 years), cardiovascular and cerebrovascular diseases (1.11 years), gastrointestinal tumors (1.31 years), lung tumors (0.63 years), other diseases (0.31 years), trauma and accidents (0.23 years), other tumors

(0.36 years), diabetes (0.07 years), and Parkinson's disease (0.01 years). These findings demonstrate that pulmonary infections, cardiovascular and cerebrovascular diseases, gastrointestinal tumors, and lung tumors have the most substantial impact on life expectancy in pneumoconiosis patients.

Important Factors Influencing the Survival Time of Pneumoconiosis Patients

Using the Cox proportional hazards regression model to analyze factors affecting pneumoconiosis patient survival time, we identified several significant predictors of mortality (P<0.05): concurrent lung tumors, concurrent lung infections, age at diagnosis, gender, pneumoconiosis stage, and dust exposure duration (Table 7). The presence of lung tumors emerged as the strongest risk factor, increasing mortality risk by 7.797-fold. Pulmonary infections substantially elevated mortality risk (relative risk=3.030), as illustrated in Figure 1. Disease stage showed a progressive relationship with mortality risk (relative risk=1.110), while male patients demonstrated a 1.186-fold higher mortality risk compared to females. Advanced age at diagnosis was associated with increased mortality risk (relative risk=1.134). Dust exposure duration showed minimal impact on survival time, with a relative risk approaching unity (0.992).

DISCUSSION

This study reveals a strong correlation between pneumoconiosis mortality and occupational distribution, with the mining sector accounting for 58.47% of cases and a predominant male patient population (93.02%). In Jiangsu Province, occupational exposure primarily involves silica and coal dust, which is reflected in the disease distribution: silicosis and coal workers' pneumoconiosis collectively

TABLE 7. Coxmodel screening of risk factors and parameter estimation for pneumoconiosis death.

Regression variables	Regression coefficient	Standard error	*Z*	*P*	Hazard ratio RR	95% *CI*	
						Upper limit	Lower limit
Diagnosed age	0.125	0.002	67.724	< 0.001	1.134	1.130	1.138
Gender	0.171	0.059	2.908	0.004	1.186	1.057	1.331
Diagnosis period	0.104	0.024	4.29	< 0.001	1.110	1.058	1.164
Dust exposure duration	−0.008	0.002	−5.088	< 0.001	0.992	0.989	0.995
pulmonary infection	1.174	0.034	34.926	< 0.001	3.236	3.030	3.456
Lung tumors	2.054	0.048	42.736	< 0.001	7.797	7.096	8.567

Note: Categorical variable assignment, gender (female=0, male=1), pulmonary infection (none=0, present=1), pulmonary tumor (none=0, present=1).
Abbreviation: CI=confidence interval, RR=relative risk.

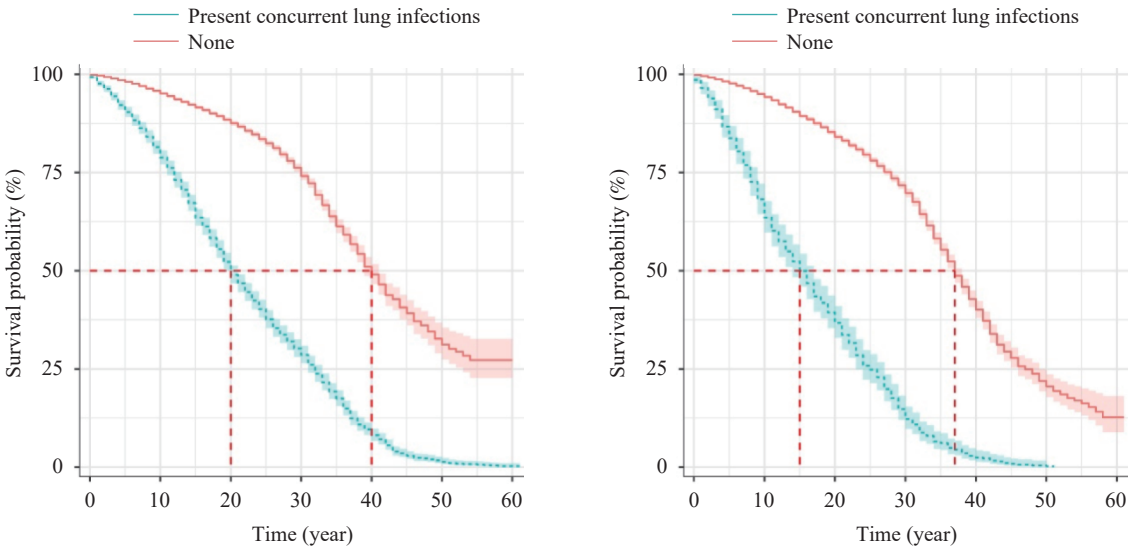

FIGURE 1. Survival curve of pneumoconiosis patients with concomitant lung infection/lung tumor.

represent 89.99% of cases. These findings emphasize the critical need for enhanced occupational health measures within high-risk industries, particularly in mining. Implementation of comprehensive occupational health protection protocols and systematic health surveillance for workers in high-risk positions is essential, with emphasis on early monitoring, protection, diagnosis, and treatment from initial exposure (*6*).

Analysis of diagnostic timing, primary mortality causes, and cause-specific mortality rates demonstrates that pulmonary infections are the predominant direct cause of death, accounting for 37.32% of cases. This finding aligns with research by Reese et al. (*7*), which identified genetic variations in telomerase reverse transcriptase and telomerase RNA components among pneumoconiosis and asbestosis patients. These telomerase gene mutations accelerate telomere shortening, exacerbating progressive fibrotic interstitial lung disease progression, altering lung architecture, and elevating infection susceptibility. The study identifies pulmonary infections, cardiovascular and cerebrovascular diseases, and gastrointestinal and lung tumors as the primary mortality causes in pneumoconiosis patients. Recent research highlights the increasing significance of cardiovascular and cerebrovascular conditions, particularly hypertension and coronary heart disease, as major public health concerns (*8*). Stage III pneumoconiosis is notably associated with severe symptomatology and poor prognosis, primarily due to complications including immunocompromise and pulmonary infections (*9*–*10*).

These findings underscore the necessity for a comprehensive management approach to pneumoconiosis treatment, emphasizing both pulmonary fibrosis management and the treatment of associated complications and chronic conditions. The statistically significant differences in diagnosis age and post-diagnosis survival time across pneumoconiosis stages ($P<0.05$) highlight the importance of thorough and timely patient evaluation, particularly for stage III patients, to address complications and reduce mortality risk.

The study's findings indicate that a substantial proportion of pneumoconiosis patients (66.03%) are diagnosed at stage I, suggesting significant potential for improving quality of life through appropriate therapeutic interventions (*11*–*12*). The identification of gastrointestinal and lung tumors as major mortality factors emphasizes the need for targeted research on improving outcomes for pneumoconiosis patients with concurrent malignancies. Life table analyses reveal that patients aged 30–34 years have an approximate life expectancy of 15.83 years. The primary factors affecting life expectancy include pulmonary infections, cardiovascular and cerebrovascular diseases, and digestive tract and lung tumors. Given that pneumoconiosis patients are typically older and often present with comorbidities such as malignancies and cardiovascular conditions, pulmonary infections represent a frequent and significant complication. These factors substantially influence both survival duration and quality of life, aligning with previous research findings (*13*–*14*). The positive nodules characteristic of pneumoconiosis not only represent typical pathological manifestations but also provide an optimal microenvironment for pathogens such as Mycobacterium tuberculosis and fungi. These nodules significantly increase infection susceptibility by compromising local immune responses. The impaired pulmonary function caused by nodules and fibrosis often leads to rapid clinical deterioration post-infection, resulting in poor therapeutic outcomes and shortened survival periods. Thus, the relationship between pulmonary infections and positive nodules may represent a primary mechanism underlying reduced life expectancy in pneumoconiosis patients. While cardiovascular and gastrointestinal diseases have less impact than pulmonary infections, they remain significant prognostic factors, possibly due to systemic effects of dust exposure, including chronic inflammatory responses. Future research exploring the relationship between positive nodules and systemic inflammatory responses may enhance our understanding of their impact on pneumoconiosis patients.

Future prevention and control strategies for pneumoconiosis should prioritize occupational health protection in high-risk industries through robust health surveillance and examination programs. While actively treating the primary condition, comprehensive management of complications and chronic comorbidities is essential. Particular attention should focus on stage III pneumoconiosis patients, ensuring thorough evaluation of all clinical parameters to facilitate early intervention for various complications. Scientific and meticulous treatment approaches, including aggressive management of pulmonary infections, cardiovascular and cerebrovascular diseases, and digestive tract and lung tumors, can potentially extend survival and enhance quality of life for the

majority of pneumoconiosis patients.

There are some limitations in this study, such as the lack of data of patients who died directly from pneumoconiosis and the failure to collect clinical data such as smoking history of patients. Future studies will improve these shortcomings.

In addition to actively treating pneumoconiosis, clinicians must prioritize the management of complications and chronic conditions. Aggressive treatment of pulmonary infections, cardiovascular and cerebrovascular diseases, and gastrointestinal and pulmonary tumors can significantly extend patient survival and enhance quality of life.

Conflicts of interest: No conflicts of interest.

Funding: Supported by the Jiangsu Provincial Science and Technology Plan Special Fund (Key R&D Program Social Development) Project (BE2022803).

doi: 10.46234/ccdcw2024.280

[#] Corresponding authors: Ming Wu, wuming@jscdc.cn; Lei Han, hanlei@jscdc.cn.

[1] Department of Epidemiology, School of Public Health, Nanjing Medical University, Nanjing City, Jiangsu Province, China; [2] The Affiliated Cancer Hospital of Nanjing Medical University, Nanjing City, Jiangsu Province, China; [3] Department of Occupation Disease Prevention and Cure, Jiangsu Provincial Center for Disease Control and Prevention, Nanjing City, Jiangsu Province, China; [4] Department of Noncommunicable Chronic Disease Control and Prevention, Jiangsu Provincial Center for Disease Control and Prevention, Nanjing City, Jiangsu Province, China.

[&] Joint first authors.

Submitted: August 14, 2024
Accepted: October 16, 2024
Issued: December 27, 2024

REFERENCES

1. Occupational Lung Disease Group of Labor Hygiene and Occupational Diseases Branch of Chinese Preventive Medicine Association. Consensus of Chinese experts on pneumoconiosis treatment (2024). J Environ Occup Med 2024;41(1):1 – 21. https://doi.org/10.11836/JEOM23379.
2. Zhou L, Han L, Xie LZ. Analysis of complications of pneumoconiosis patients in Jiangsu Province from 2006 to 2017. Ind Health Occup Dis 2021;47(2):97-9. https://d.wanfangdata.com.cn/periodical/gywsyzyb202102003. (In Chinese).
3. Xie LZ, Zhou L, Zhao Y, Liu J, Wang W, Zhang W, et al. Follow-up and retrospective investigation of patients with pneumoconiosis in Jiangsu Province, China. Chin Ind Hyg Occup Dis 2020;38(4):251 – 5. https://doi.org/10.3760/cma.j.cn121094-20191115-00530.
4. World Health Organization. International statistical classification of diseases and related health problems. Beijing Union Medical College Hospital World Health Organization International Classification Family Cooperation Center, trans. 2nd ed. Beijing: People's Medical Publishing House. 2016; p. 20. https://book.kongfz.com/399379/7575586286. (In Chinese).
5. Fang JQ. Health statistics. Beijing: People's Health Publishing House. 2016; p. 369-375.
6. Zhou L, Han L, Zhao Y, Gao QQ, Zhou P, Xie LZ. Results of active surveillance and medical follow-up of pneumoconiosis in Jiangsu Province during 2019 to 2022. Occup Health Emerg Rescue 2024;42(2):192 – 6. https://doi.org/10.16369/j.oher.issn.1007-1326.2024.02.009.
7. Rees D, Murray J. Silica, silicosis and tuberculosis. Int J Tuberc Lung Dis 2007;11(5):474-84. https://pubmed.ncbi.nlm.nih.gov/17439668/.
8. Xu PL, Murizhati·Maimaiti, Zikeya·Naijimu, Sun H, Wei JJ, Wang X. Investigation on status quo of chronic disease spectrum of residentsin Xinjiang and its countermeasures. Soft Sci Health 2021;35(2):73 – 6. https://doi.org/10.3969/j.issn.1003-2800.2021.02.018.
9. Chen ZD, Mao L, Wen J, Zhou SW, Liu MQ, Yuan HL. Report of a case with stage III silicosis, pneumonia complicated with pulmonary embolism. Occup Health Emerg Rescue 2021;39(4):463 – 4,471. https://doi.org/10.16369/j.oher.issn.1007-1326.2021.04.022.
10. Zheng BN, Liu HT, Liang HD, Du YH, Lu JH. Analysis of influencing factors of pneumoconiosis complicated with pulmonary tuberculosis. Chin Ind Hyg Occup Dis 2021;39(7):519 – 22. https://doi.org/10.3760/cma.j.cn121094-20200820-00479.
11. Sun BQ, Zhao HL, Xie Y. Progress in epidemiological studies on pneumoconiosis with comorbidities. Chin Ind Hyg Occup Dis 2021;39(5):389 – 93. https://doi.org/10.3760/cma.j.cn121094-20200601-00306.
12. Sarı G, Şimşek C. A descriptive study of a Turkish pneumoconiosis case-series. Med Lav 2023;114(1):e2023003. https://doi.org/10.23749/mdl.v114i1.13215.
13. Altınöz H, Çelikkalkan C, Horasan GD, Hamşioğlu F, Cengiz N, Orbay H. Socio-demographic and clinical characteristics of turkish workers with pneumoconiosis. Cent Eur J Public Health 2016;24(3):231 – 3. https://doi.org/10.21101/cejph.a4694.
14. Zhou L, Xie LZ, Han L. Analysis of causes of death in 2567 cases of pneumoconiosis in Jiangsu Province. Mod Prev Med 2022;49(12):2159-63,2177. https://d.wanfangdata.com.cn/periodical/xdyfyx202212009. (In Chinese).

Youth Editorial Board

Indexed by Science Citation Index Expanded (SCIE), Social Sciences Citation Index (SSCI), PubMed Central (PMC), Scopus, Chinese Scientific and Technical Papers and Citations, and Chinese Science Citation Database (CSCD)

The inauguration of *China CDC Weekly* is in part supported by Project for Enhancing International Impact of China STM Journals Category D (PIIJ2-D-04-(2018)) of China Association for Science and Technology (CAST).

CCDC weekly

Vol. 6 No. 52 Dec. 27, 2024

Responsible Authority
National Disease Control and Prevention Administration

Sponsor
Chinese Center for Disease Control and Prevention

Editing and Publishing
China CDC Weekly Editorial Office
No.155 Changbai Road, Changping District, Beijing, China
Tel: 86-10-63150501, 63150701
Email: weekly@chinacdc.cn

CSSN
ISSN 2096-7071 (Print)
ISSN 2096-3101 (Online)
CN 10-1629/R1